102 Wolbank S, Peterbauer A, Wassermann E et al. Labelling of human adipose-derived stem cells for non-invasive in vivo cell tracking. Cell Tissue Bank 2006;8:163–177.
103 Hofmann M, Wollert KC, Meyer GP et al. Monitoring of bone marrow cell homing into the infarcted human myocardium. Circulation 2005; 111:2198–2202.
104 Kraitchman DL, Heldman AW, Atalar E et al. In vivo magnetic resonance imaging of mesenchymal stem cells in myocardial infarction. Circulation 2003;107:2290–2293.
105 Contag CH, Contag PR, Mullins JI et al. Photonic detection of bacterial pathogens in living hosts. Mol Microbiol 1995;18:593–603.
106 Brychta P. EATB: Standards for banking of biologic skin substitutes (BSS). Cell Tissue Bank 2002;3:59–71.
107 Cobo F, Cabrera C, Catalina P et al. General safety guidances in stem cell bank installations. Cytotherapy 2006;8:47–56.
108 Common Standards for Tissue and Cell Banking (EATB, EAMST, EEBA). Available at http://www.eatb.de. Accessed May 15, 2007.
109 EudraLex. Volume 4. Medicinal Products for Human and Veterinary Use: Good Manufacturing Practice. Available at http://ec.europa.eu/enterprise/pharmaceuticals/homev4.htm. Accessed May 15, 2007.
110 Chrysler GR, McKenna DH, T S et al. Cord Blood Banking. In: Broxmeyer HE, ed. Cord blood: Biology, immunology, banking and clinical transplantation. Bethesda, MD: AABB Press, 2004;219–257.
111 Lapierre V, Pellegrini N, Bardey I et al. Cord blood volume reduction using an automated system (Sepax) vs. a semi-automated system (Optipress II) and a manual method (hydroxyethyl starch sedimentation) for routine cord blood banking: A comparative study. Cytotherapy 2007;9: 165–169.
112 Skoric D, Balint B, Petakov M et al. Collection strategies and cryopreservation of umbilical cord blood. Transfus Med 2007;17:107–113.
113 Broxmeyer HE, Douglas GW, Hangoc G et al. Human umbilical cord blood as a potential source of transplantable hematopoietic stem/progenitor cells. Proc Natl Acad Sci U S A 1989;86:3828–3832.
114 Gluckman E, Broxmeyer HA, Auerbach AD et al. Hematopoietic reconstitution in a patient with Fanconi's anemia by means of umbilical-cord blood from an HLA-identical sibling. N Engl J Med 1989;321:1174–1178.
115 Parolini O, Soncini M. Human placenta: A source of progenitor/stem cells? J Reprod Med Endocrinol 2006;3(2):117–126.
116 Davis JW. Skin transplantation with a review of 550 cases at the Johns Hopkins Hospital. Johns Hopkins Med J 1910;15:307–396.
117 Stern W. The grafting of preserved amniotic membrane to burned and ulcerated skin. JAMA 1913;13:973–974.
118 Sabella W. Use of fetal membranes in skin grafting. Med Rec NY 1913;83:478–480.
119 de Roth A. Plastic repair of conjunctival defects with fetal membranes. Arch Ophthalmol 1940;23:522–525.
120 Kim JC, Tseng SC. Transplantation of preserved human amniotic membrane for surface reconstruction in severely damaged rabbit corneas. Cornea 1995;14:473–484.
121 Tosi GM, Massaro-Giordano M, Caporossi A et al. Amniotic membrane transplantation in ocular surface disorders. J Cell Physiol 2005;202:849–851.
122 Gansira MA. Amniotic membrane in surgery. J Pak Med Assoc 2003; 53:29–32.
123 Dua HS, Gomes JA, King AJ et al. The amniotic membrane in ophthalmology. Surv Ophthalmol 2004;49:51–77.
124 Hao Y, Ma DH, Hwang DG et al. Identification of antiangiogenic and antiinflammatory proteins in human amniotic membrane. Cornea 2000; 19:348–352.
125 Tseng SC, Prabhasawat P, Lee SH. Amniotic membrane transplantation for conjunctival surface reconstruction. Am J Ophthalmol 1997;124: 765–774.
126 Ravishanker R, Bath AS, Roy R. "Amnion Bank"—The use of long term glycerol preserved amniotic membranes in the management of superficial and superficial partial thickness burns. Burns 2003;29: 369–374.
127 Burman S, Tejwani S, Vemuganti GK et al. Ophthalmic applications of preserved human amniotic membrane: A review of current indications. Cell Tissue Bank 2004;5:161–175.
128 Branski L, Jeschke M, Celis M et al. The treatment of partial thickness burns: Amnion versus topical antimicrobial creme. J Surg Res 2006; 130:276–277.
129 Hennerbichler S, Reichl B, Pleiner D et al. The influence of various storage conditions on cell viability in amniotic membrane. Cell Tissue Bank 2007;8:1–8.
130 Hennerbichler S, Reichl B, Wolbank S et al. Cryopreserved amniotic membrane releases angiogenic factors. Wound Rep Reg 2007;15: A51.
131 Branski L, Kulp G, Jeschke M et al. Amniotic membrane as wound coverage: The effects of irradiation and different processing methods on growth factor content. J Surg Res 2007;137:339.
132 Heeger PS. Amnion and chorion cells as therapeutic agents for transplantation and tissue regeneration: A field in its infancy. Transplantation 2004;78:1411–1412.
133 Ilancheran S, Michalska A, Peh G et al. Stem cells derived from human fetal membranes display multi-lineage differentiation potential. Biol Reprod 2007;77:577–588.
134 Battula VL, Bareiss PM, Treml S et al. Human placenta and bone marrow derived MSC cultured in serum-free, b-FGF-containing medium express cell surface frizzled-9 and SSEA-4 and give rise to multilineage differentiation. Differentiation 2007;75:279–291.

Immunology

Expansion of Vα24$^+$Vβ11$^+$ NKT cells from cord blood mononuclear cells using IL-15, IL-7 and Flt3-L depends on monocytes

Hikaru Okada[*1], *Tokiko Nagamura-Inoue*[1,2], *Yuka Mori*[1] *and Tsuneo A. Takahashi*[1]

[1] Division of Cell Processing, Research Hospital, Institute of Medical Science, University of Tokyo, Tokyo, Japan
[2] Department of Cell Processing and Transfusion, Research Hospital, Institute of Medical Science, University of Tokyo, Tokyo, Japan

Human Vα24$^+$Vβ11$^+$ NKT cells are a unique T cell population specifically and potently activated by α-galactosylceramide (αGalCer, KRN7000) presented by CD1d. Here, we present a simple and efficient method for expanding Vα24$^+$Vβ11$^+$ NKT cells from human cord blood mononuclear cells (CBMNC) using αGalCer in the presence of interleukin (IL)-15, IL-7 and Flt3-L. The addition of αGalCer from day 0, compared to its addition from day 8 or day 15, induced a greater expansion of NKT cells. The maximal expansion of NKT cells was observed after 15 days (2300-fold). Thereafter, the number of NKT cells decreased slowly, a decrease that was correlated with the diminution of CD1d-positive cells. NKT cell proliferation induced by αGalCer was not observed when CD1d-expressing monocytes were depleted from CBMNC, whereas B cell and dendritic cell depletions had no effect. Expanded NKT cells were CD4$^+$CD8$^-$ and secreted both IL-4 and IFN-γ. In this system, CD3$^+$ T cells and CD3$^-$CD56$^+$ NK cells were also expanded. However, the expansion of NKT cells had no significant functional effect on T and NK cells. This expansion method of CBMNC-derived NKT cells is simple and may be helpful for clinical use.

Received 9/2/05
Revised 15/9/05
Accepted 9/11/05

[DOI 10.1002/eji.200526085]

Key words: α-Galactosylceramide · Cord blood · Expansion · Human · Vα24$^+$Vβ11$^+$ NKT cells

Introduction

Natural killer T (NKT) cells correspond to a novel T cell population with an invariant TCR that recognizes glycolipids presented by CD1d, an MHC-like molecule well conserved between humans and mice [1–3]. Many studies have described the potential anti-tumor effect [4–7] and the immunoregulatory function of NKT cells [8–11]. Vα24$^+$Vβ11$^+$ NKT cells, the human counterpart of mouse Vα14$^+$Vβ8.2$^+$ NKT cells, are limited to a small lymphocyte subpopulation [12] that can be selectively activated by α-galactosylceramide (αGalCer; KRN7000) presented by CD1d [13, 14]. Takahashi *et al.* and others showed that they proliferate in response to dendritic cells (DC) once pulsed by αGalCer [15, 16]. Several cytokines were used in attempt to expand and activate NKT cells from human peripheral blood [17–19], and recently from human cord blood [20, 21]. Interleukin (IL)-2 is one of the classical cytokines used to expand and stimulate NKT cells [22]. Here, we describe a

Correspondence: Tsuneo A. Takahashi, Division of Cell Processing, Institute of Medical Science, University of Tokyo, 4-6-1, Shirokanedai, Minato-ku, Tokyo, 108-8639, Japan
Fax: +81-3-54495452
e-mail: takahasi@ims.u-tokyo.ac.jp

Abbreviations: **αGalCer:** α-galactosylceramide · **βGalCer:** β-galactosylceramide · **CBMNC:** cord blood mononuclear cell · **CBT:** cord blood transplantation · **GVHD:** graft-*versus*-host disease · **GVL:** graft-*versus*-leukemia

* Current address: Central Laboratory of Hematology, Centre Hospitalier Universitaire Vaudois, Bugnon 46, 1011 Lausanne, Switzerland.

Table 1. Cell compartments of CBMNC before and after culture[a)]

Cord Blood	T cells ($CD3^+$)	NK cells	B cells	Monocytes	DC
Day 0	15.0 ± 9.6	19.9 ± 10.3	10.2 ± 4.4	32.4 ± 7.6	0.04 ± 0.02
Day 8	74.6 ± 8.1	20.7 ± 8.2	2.16 ± 0.01	0.16 ± 0.01	0.11 ± 0.01
Day 15	86.2 ± 8.6	13.1 ± 9.0	ND	ND	ND

a) Cells were cultured in the presence of 50 ng/mL IL-15, 10 ng/mL IL-7, 10 ng/mL Flt3-L and 100 ng/mL αGalCer from day 0. Data shown are the means ± SD of ten samples (% of CBMNC). ND: not determined.

combination of IL-15, IL-7 and Flt3-ligand (Flt3-L) to expand NKT cells from human cord blood mononuclear cells (CBMNC). IL-15 is a newly cloned cytokine that promotes T cell proliferation and NK cell activation [23]. In fact, in IL-$15^{-/-}$ and IL-$15R\alpha^{-/-}$ mice, NK and NKT cell counts are diminished [24, 25]. IL-7 is a potent lymphoid growth factor that is important for T cell proliferation and survival as well as for NK cell function [26]. Flt3-L induces hematopoietic stem cell proliferation and early lymphopoiesis. In addition, we have previously shown that a high concentration of IL-15 (50 ng/mL), together with 10 ng/mL of Flt3-L, efficiently expands $CD3^+$ T cells derived from human CBMNC [27].

Cord blood is a source of stem cells currently used for transplantation. Several aspects of unrelated cord blood transplantation (CBT) differ from bone marrow or peripheral blood stem cell transplantation. As many as two HLA mismatches are acceptable in CBT for successful engraftment with only a mild graft-*versus*-host disease (GVHD) [28], because cord blood T cells are immature and naive compared to peripheral blood lymphocytes. The relationship between lower risk of GVHD and higher risk of leukemic relapse is well known, and a higher risk of relapse in CBT was expected. Surprisingly, unrelated CBT and unrelated bone marrow transplantation had a comparable relapse rate in adults as well as in children [29, 30]. However, the major causes of death in CBT in adults were relapse of the disease and infections due to delayed hematopoietic recovery [30, 31]. As $V\alpha24^+V\beta11^+$ NKT cells produce both Th1 and Th2 cytokines upon activation, they may have an immunomodulatory effect that could abolish GVHD without affecting the graft-*versus*-leukemia (GVL) effect [32, 33].

Here, we present a simple and efficient method for expanding $V\alpha24^+V\beta11^+$ NKT cells derived from human CBMNC. Moreover, we observed that monocytes are critical for $V\alpha24^+V\beta11^+$ NKT cell expansion. Expansion of T lymphocytes and NK cells was also observed. Expanded $V\alpha24^+V\beta11^+$ NKT cells had a $CD4^+CD8^-$ phenotype and secreted both IL-4 and IFN-γ. Observations presented here may be helpful for a more targeted use of human cord blood in immunotherapy.

Results

Phenotypic analysis of lymphocytes in human cord blood

After separation by Ficoll density gradient centrifugation, $CD3^+$ T cells varied in fresh CBMNC from 2.5 to 36.2% (mean 15.0 ± 9.6%, $n = 10$). Other cell compartments consisted of 19.9 ± 10.3% $CD3^-CD56^+$ NK cells, 10.2 ± 4.4% $CD19^+$ B cells, 32.4 ± 7.6% $CD14^+$ monocytes and only 0.04 ± 0.02% $CD3^-CD1a^+$ DC as shown in Table 1 (day 0). The majority of $CD3^+$ T cells were $TCR\alpha\beta^+$ (97.0 ± 2.1%) and 3.0 ± 2.1% were $TCR\gamma\delta^+$. Of T cells, 75.8 ± 14.1% were $CD4^+CD8^-$ (CD4 single-positive cells), 18.2 ± 9.5% $CD4^-CD8^+$ (CD8 single-positive cells), 2.5 ± 2.5% $CD4^+CD8^+$ (double-positive cells) and 1.1 ± 0.9% $CD4^-CD8^-$ (double-negative cells) (Table 2, day 0). Only 0.04 ± 0.03% of $CD3^+$ T cells were $V\alpha24^+V\beta11^+$ NKT cells (Table 2).

Cytokine combination for cell expansion

Because NKT cells, and especially $V\alpha24^+V\beta11^+$ NKT cells, represent a very small population of T cells, we

Table 2. T cell phenotypes in CBMNC before and after culture[a)]

	$TCR\alpha\beta^+$	$TCR\gamma\delta^+$	$CD4^+CD8^-$	$CD4^-CD8^+$	$CD4^+CD8^+$	$CD4^-CD8^-$	$V\alpha24^+V\beta11^+$ NKT
Day 0	97.0 ± 2.1	3.0 ± 2.1	75.8 ± 14.1	18.2 ± 9.5	2.5 ± 2.5	1.1 ± 0.9	0.04 ± 0.03
Day 8	95.2 ± 0.8	5.3 ± 1.4	66.1 ± 12.1	29.6 ± 10.7	0.6 ± 0.1	3.7 ± 1.8	0.8 ± 0.6
Day 15	91.9 ± 1.6	8.0 ± 0.9	60.8 ± 9.6	31.4 ± 11.2	4.4 ± 1.1	3.4 ± 0.5	3.7 ± 0.3

a) Cells were cultured under the same condition as in Table 1. Data shown are the means ± SD of six samples (% of $CD3^+$ T cells).

chose to expand CBMNC rather than sorting $V\alpha24^+V\beta11^+$ NKT cells. Previously, Nagamura-Inoue *et al.* found that a high concentration of IL-15 (50 ng/mL), together with 10 ng/mL Flt3-L, efficiently expanded $CD3^+$ T cells derived from CBMNC [27]. In addition, IL-7 is one of the growth factors needed to expand and activate T cells [26]. Therefore, we compared different combinations of these three cytokines (50 ng/mL IL-15, 10 ng/mL IL-7 and/or 10 ng/mL Flt3-L). Results are shown in Fig. 1. In the absence of cytokines or in the presence of Flt3-L alone, $CD3^+$ T cells and NK cells diminished by day 15, and the remaining cells were $CD3^-CD56^-$. IL-7 at 10 ng/mL only resulted in 2.3-fold expansion of T cells. A significant synergistic induction of $CD3^+$ T cells was observed with a combination of 50 ng/mL IL-15, 10 ng/mL IL-7 and 10 ng/mL Flt3-L (14.1-fold induction). However, even by combining these three cytokines, no increase of $V\alpha24^+V\beta11^+$ NKT cells was observed unless αGalCer was added.

CD1d-expressing cells in human cord blood

Since $V\alpha24^+V\beta11^+$ NKT cell activation is CD1d dependent, we examined whether antigen-presenting cells like monocytes ($CD14^+$), B cells ($CD19^+$) and DC ($CD3^-CD1a^+$) expressed CD1d in fresh CBMNC. As shown in Fig. 2A, the majority of CD1d-positive cells were observed among $CD14^+$ monocytes, whereas $CD19^+$ B cells did not strongly express CD1d and only 0.01% of $CD3^-CD1a^+$ DC were $CD1d^+$ among human CBMNC. By day 8 in the presence of IL-15, IL-7 and Flt3-L, $CD1d^+$ cells decreased as shown in Table 1 (day 8). In addition, the remaining B cells, monocytes and the few DC no longer expressed CD1d (Fig. 2A, right panels).

Expansion of NKT cells from human cord blood

IL-15 is a cytokine that has been reported to induce monocyte differentiation into mature DC [34]. In order to explore whether DC maturation could enhance $V\alpha24^+V\beta11^+$ NKT cell expansion, αGalCer was directly added to CBMNC cultured with IL-15, IL-7 and Flt3-L from day 0, day 8 or day 15. The addition of αGalCer from day 0 induced a significantly greater $V\alpha24^+V\beta11^+$ NKT cell expansion than the addition of αGalCer from day 8 or day 15 (Fig. 2B). After 15 days of culture, the absolute number of $V\alpha24^+V\beta11^+$ NKT cells pulsed with αGalCer was 2300 ± 1200-fold higher than that observed in fresh CBMNC (Fig. 2B). $CD3^+$ T cells and NK cells were also expanded 27 ± 15-fold and 2 ± 1-fold, respectively, compared to the pre-cultured population (Fig. 2C). $CD3^+$ T cells and NK cells represent 86.2 ± 8.6% and 13.1 ± 9.0%, respectively, of total cultured CBMNC on day 15 (Table 1, day 15). In control experiments, β-galactosylceramide (βGalCer) did not induce $V\alpha24^+V\beta11^+$ NKT cell proliferation, while the T cells or NK cells presented almost the same expansion rate. As described above, the $CD3^-CD56^-$ fraction nearly disappeared on day 8 (Fig. 2C). Maximal expansion of $V\alpha24^+V\beta11^+$ NKT cells was observed after 15 days of culture. Thereafter, the absolute number of $V\alpha24^+V\beta11^+$ NKT cells slowly decreased, a phenomenon that followed the reduction of $CD1d^+$ cells (Table 1, Fig. 2A).

Depletion of antigen-presenting cells

Because $V\alpha24^+V\beta11^+$ NKT cells could only be expanded in the presence of αGalCer, we next tried to detect which $CD1d^+$ cells in the CBMNC were critical for the

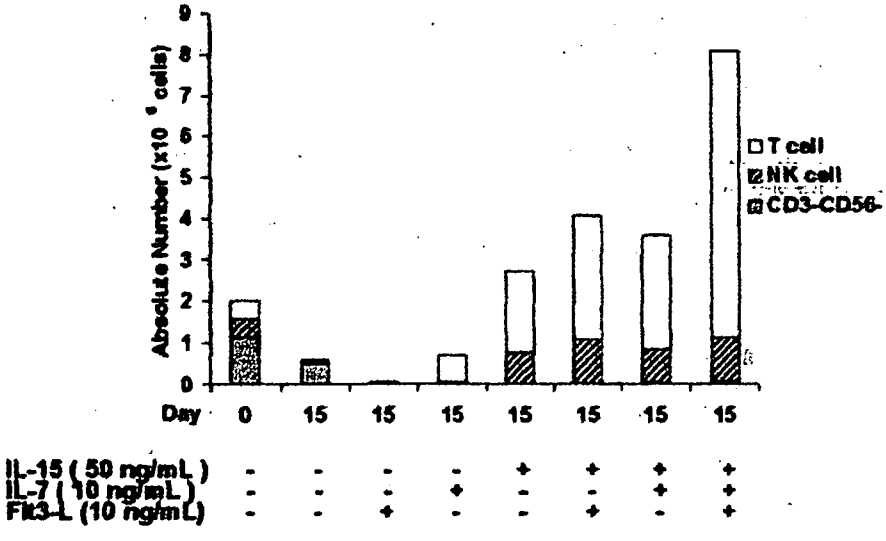

Figure 1. Comparison of cell compartments in fresh CBMNC (day 0) and after 15 days of culture with different combinations of 50 ng/mL IL-15, 10 ng/mL IL-7 and 10 ng/mL Flt3-L.

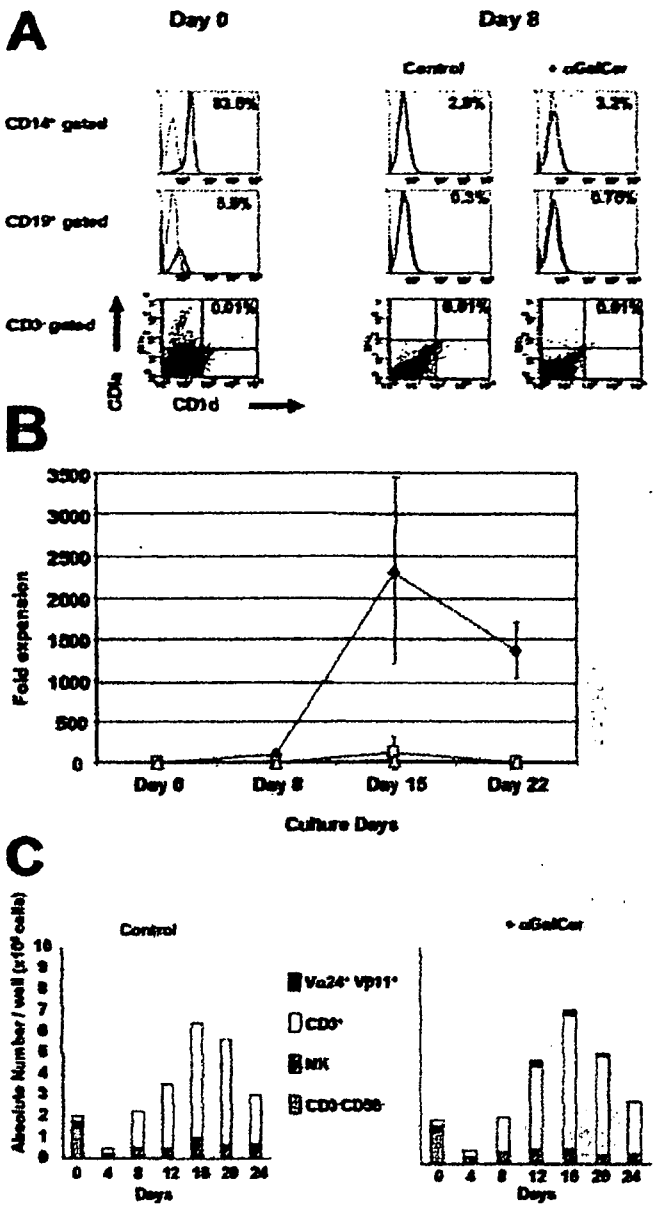

Figure 2. (A) CD1d expression on $CD14^+$ monocytes, $CD19^+$ B cells and $CD3^-CD1a^+$ DC in freshly isolated CBMNC (left panel, day 0) and after 8 days of culture with 50 ng/mL IL-15, 10 ng/mL IL-7 and 10 ng/mL Flt3-L in the presence or absence of αGalCer from day 0 (right panels, day 8). Isotype control is represented with a dashed line and CD1d-positive cells with a solid line for $CD14^+$- and $CD19^+$-gated cells. $CD3^-$ cells are gated in the dot blots and $CD3^-CD1a^+CD1d^+$ cells represented only 0.01% of the $CD3^-CD1a^+$ cells. (B) Fold expansion of $V\alpha24^+V\beta11^+$ NKT cells. αGalCer (100 ng/mL) was added to the CBMNC from day 0 (◆), day 8 (□) or day 15 (△) in the presence of 50 ng/mL IL-15, 10 ng/mL IL-7 and 10 ng/mL Flt3-L. The fold expansion represents the ratio of the absolute number of NKT cells per well after culture to the number at day 0. (C) Cell compartments of CBMNC in the presence or absence of αGalCer. CBMNC were cultured with 50 ng/mL IL-15, 10 ng/mL IL-7 and 10 ng/mL Flt3-L. αGalCer was added to the medium at a concentration of 100 ng/mL from day 0 (right panel). βGalCer was used in a control experiment (left panel).

expansion of $V\alpha24^+V\beta11^+$ NKT cells. CBMNC were depleted of either $CD14^+$ monocytes, $CD19^+$ B cells, $CD1a^+$ DC, or of all of these three antigen-presenting cells. Then, depleted cells were individually cultured in the presence of IL-15, IL-7 and Flt3-L as described above and pulsed with 100 ng/mL αGalCer from day 0. The absolute number of $V\alpha24^+V\beta11^+$ NKT cells was calculated as described in Materials and methods. When $CD14^+$ monocytes were depleted, the $V\alpha24^+V\beta11^+$ NKT cells did not proliferate, as shown in Fig. 3. In contrast, depletion of $CD19^+$ B cells or $CD1a^+$ DC had no significant influence on the proliferation of $V\alpha24^+V\beta11^+$ NKT cells.

Phenotypic analysis of expanded $V\alpha24^+V\beta11^+$ NKT cells and $CD3^+$ T cells

CBMNC were cultured with IL-15, IL-7, Flt3-L and 100 ng/mL αGalCer. After 15 days, $CD3^+$ T cells represented 86.2 ± 8.6% of the mononuclear cells and the remaining population was constituted by NK cells (13.1 ± 9.0%) (Table 1). Expanded $V\alpha24^+V\beta11^+$ NKT cells represented 3.7 ± 0.3% of the $CD3^+$ T cells (Fig. 4A, lower part). Most of the $V\alpha24^+$ NKT cells were positive for CD4 (95.6 ± 5.1%) and very few expressed CD8 (1.1 ± 1.1%) (n = 5). In addition, 1.8% $V\alpha24^+$ NKT cells were double negative ($CD4^-CD8^-$). Of the other $CD3^+$ T cells in cultured cells, 60.8 ± 9.6% were $CD4^+$, 31.4 ± 11.2% $CD8^+$, 4.4 ± 1.1% $CD4^+CD8^+$, 3.4 ± 0.54% $CD4^-CD8^-$ (Table 2, day 15) and 23.8 ± 7.9% of $CD3^+$ T cells were $CD56^+$ (n = 6). In the absence of αGalCer, $V\alpha24^+V\beta11^+$ NKT cells were not

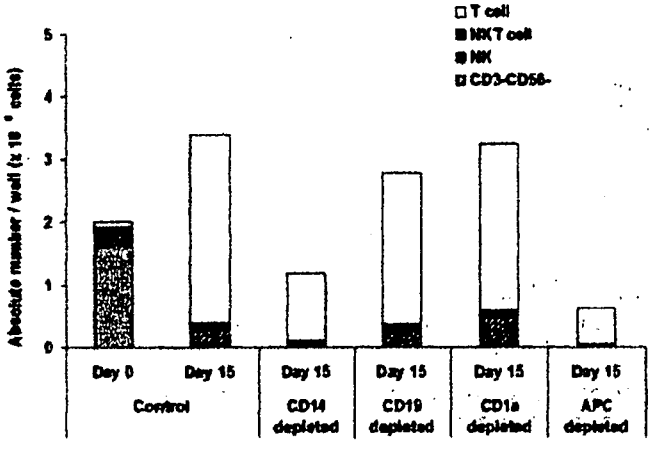

Figure 3. Depletion of CD1d-expressing cells. Either $CD14^+$ monocytes, $CD19^+$ B cells, $CD1a^+$ DC or all of these three antigen-presenting cells (APC) were depleted from CBMNC using AutoMACS beads. After depletion, the remaining cells were cultured with 50 ng/mL IL-15, 10 ng/mL IL-7, 10 ng/mL Flt3-L and 100 ng/mL αGalCer for 15 days. One representative result from three independent experiments is shown.

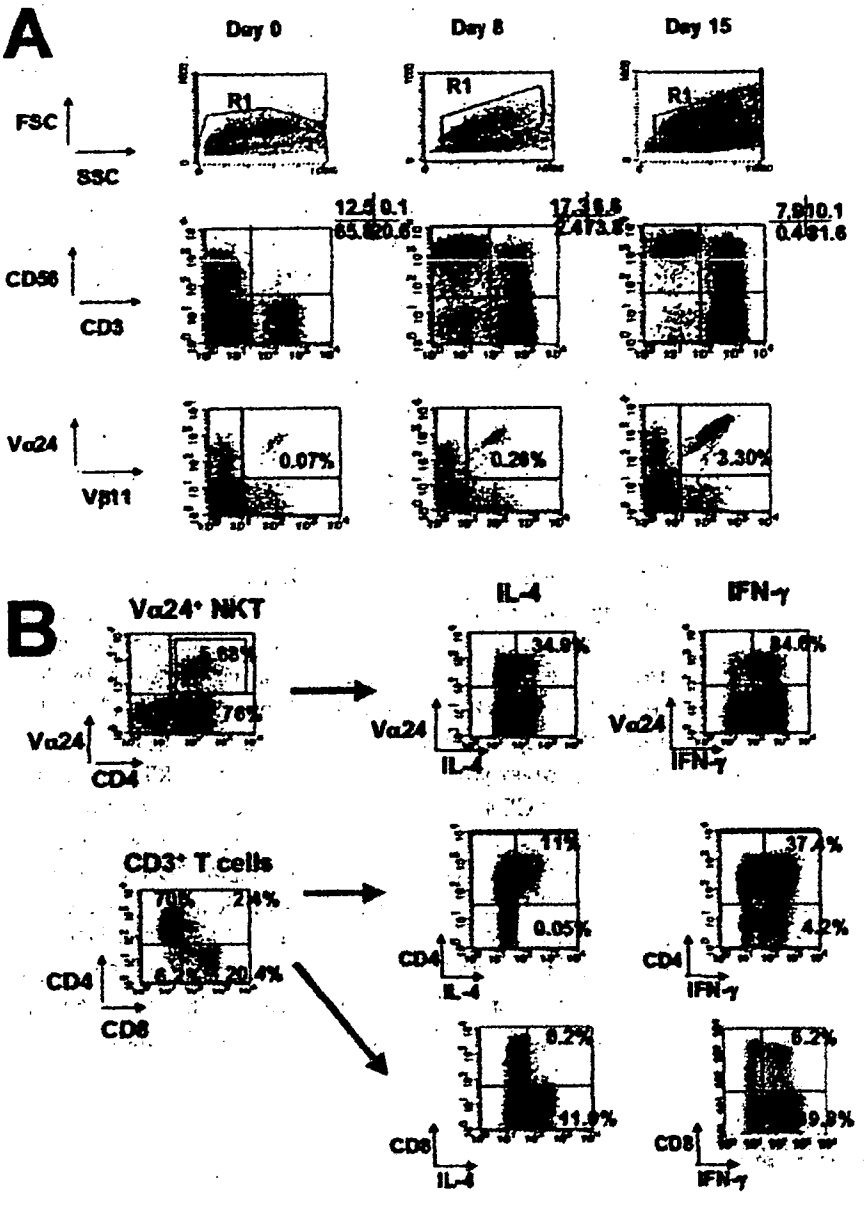

Figure 4. (A) Percentages of T and NK cells (R1 gated; middle part) and Vα24$^+$Vβ11$^+$ NKT cells (CD3$^+$ T cell gated; lower part) at day 0 and after 8 or 15 days of culture with IL-15, IL-7, Flt3-L and αGalCer from day 0. (B) IL-4 and IFN-γ secretion by cultured Vα24$^+$Vβ11$^+$ NKT cells (CD4$^+$ gated) and other T cell compartments. On day 15, the expanded CD4$^+$ single-positive Vα24$^+$Vβ11$^+$ NKT cells produced IL-4 and also IFN-γ (upper part). The remaining post-cultured CD4$^+$ T cells also produced IL-4 and IFN-γ, whereas CD8$^+$ T cells secreted IFN-γ alone (lower part). Control experiment was made without stimulation with PMA and ionomycin.

detected, but CD3$^+$ T cells showed the same phenotype as in the presence of αGalCer (data not shown).

Cytokine secretion profile of expanded Vα24$^+$Vβ11$^+$ NKT cells

Cytokine secretion of expanded Vα24$^+$Vβ11$^+$ NKT cells was investigated by examining the intracellular expression of IFN-γ as Th1 cytokine and of IL-4 as Th2 cytokine. On day 15, the expanded CD4$^+$ single-positive Vα24$^+$Vβ11$^+$ NKT cells produced both IL-4 and IFN-γ (Fig. 4B). CD4$^+$ T cells produced both IL-4 and IFN-γ, while CD8$^+$ T cells secreted IFN-γ only. On the other hand, without expansion of CD4$^+$ Vα24$^+$Vβ11$^+$ NKT cells by αGalCer, the CD4/CD8 ratio and the cytokine secretion of T cells did not change significantly (data not shown).

Cytotoxic activity against K562 cells

We evaluated the effect of Vα24$^+$Vβ11$^+$ NKT cells on the cytotoxic activity of the cultured CBMNC against K562 cells, an erythroleukemic cell line, as described in Materials and methods. Fresh CBMNC showed a

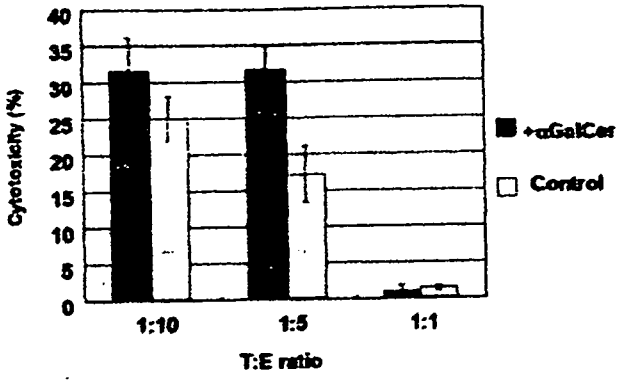

Figure 5. Comparison of the cytotoxic activity of the cultured CBMNC against K562 cells. On day 15, cells cultured in the presence (filled bar) or absence (open bar) of αGalCer were examined for their cytotoxic activity against K562 cells. The effector cells (E) and target cells (T) were mixed to obtain T : E ratios of 1 : 10, 1 : 5 and 1 : 1. One representative of three independent experiments is shown.

minimal cytotoxic activity against K562 cells, while cells cultured for 15 days with αGalCer gained in cytotoxic activity. The CBMNC cultured with αGalCer had an enhanced cytotoxicity against K562 cells compared to the control, but had no significant additive effect on the cytotoxic activity of NK and T cells (p = not significant) (Fig. 5).

Discussion

In the present study, we succeeded in expanding $V\alpha24^+V\beta11^+$ NKT cells from human CBMNC without losing progenitor cells by cell sorting. The expanded $V\alpha24^+V\beta11^+$ NKT cells presented a $CD4^+$ single-positive phenotype and secreted both IL-4 and IFN-γ.

Similarly to mouse $V\alpha14^+V\beta8.2^+$ NKT cells, the activation and proliferation of human $V\alpha24^+V\beta11^+$ NKT cells are CD1d dependent. Previous reports used DC as the strongest antigen-presenting cells for the expansion of $V\alpha24^+V\beta11^+$ NKT cells in adult peripheral blood [18, 19] and in cord blood [20]. However, to avoid the loss of any cell compartments through additional manipulations, we describe here a method to easily expand $V\alpha24^+V\beta11^+$ NKT cells in the presence of IL-15, IL-7 and Flt3-L without DC induction.

Ueda *et al.* succeeded in expanding $V\alpha24^+V\beta11^+$ NKT cells by adding αGalCer directly to fresh CBMNC in the presence of IL-2 [22]. IL-15 has been recently reported as one of the cytokines involved in monocyte differentiation into mature DC, the strongest antigen-presenting cells [34, 35]. In our system, we observed a 2300-fold expansion of $V\alpha24^+V\beta11^+$ NKT cells after 15 days, although DC did neither proliferate nor maturate.

According to the results of our depletion analysis, monocytes constituted the $CD1d^+$ cell compartment critically involved in NKT cell expansion, whereas B cells and DC were not required. $CD4^+$ $V\alpha24^+V\beta11^+$ NKT cells did not proliferate for more than 15 days in the presence of IL-15, IL-7, Flt3-L and αGalCer. This phenomenon seemed to be correlated with the decrease of the CD1d-presenting cells.

The complexity of the NKT cell phenotype in mice was emphasized by several classifications [36]. Using CD1d tetramers loaded with αGalCer, four subsets of NKT cells were identified, differing in NK1.1 expression, TCR repertoire and CD1d-dependence [37, 38]. These different subsets might explain the paradoxical properties of NKT cells, as CD1d-restricted NKT cells inhibited tumor growth in some cases, but could also suppress anti-tumor immunity in other experiments [12, 39]. Although mouse CD1d-αGalCer tetramers stained human NKT cells, further studies are required to characterize human NKT cell specificities. In our system, expanded $V\alpha24^+V\beta11^+$ NKT cells were CD4 single positive and produced both IL-4 and IFN-γ. IL-7 up-regulates IL-4 production by NKT cells in mice [40], but we did not observe any Th2 polarization despite the presence of IL-7 in the culture medium. Lin *et al.* have tested different cytokines to expand NKT cells from peripheral blood mononuclear cells [16]. IL-2 and IL-15 resulted in the best expansion rate, and IL-15 enhanced the cytotoxic activity of NKT cells against U937 cells after 7 days of culture. Both IL-7 and IL-15 preferentially expanded $CD4^-CD8^-$ NKT cells, and the authors proposed to combine those two cytokines for an optimal anti-tumor application of NKT cells. However, in our study, $CD4^+$ NKT cells were predominant when CBMNC were expanded with IL-15, IL-7 and Flt3-L, and they produced both Th1 and Th2 cytokines. Cord blood-derived NKT cells may have specific properties compared to peripheral blood-derived NKT cells.

Whether human $V\alpha24^+V\beta11^+$ NKT cells exhibit direct cytotoxic activity is still controversial [41]. Because $V\alpha24^+V\beta11^+$ NKT cells produce huge amounts of cytokines rapidly after αGalCer stimulation, they may act preferentially by stimulating other effector cells such as NK or CD8 T cells. In our system, the cytotoxicity of CBMNC against K562 cells was enhanced after 15 days of culture. However, the $V\alpha24^+V\beta11^+$ NKT cell expansion did not enhance the cytotoxicity of NK cells. As $CD4^+$ NKT cells produce both Th1 and Th2 cytokines, they may not influence the anti-tumoral response of NK cells. The culture of CBMNC with or without αGalCer did not change T and NK cell compartments either. The CD4/CD8 ratio remained stable, as was the cytokine profile of $CD4^+$ and $CD8^+$ T cells (data not shown).

The role of NK cells in acute GVHD and the GVL effect may be as important as that of T cells [42]. In our

system, the fact that $CD8^+$ T and NK cells increased significantly after 15 days of culture might result in enhancing not only the GVL effect but also GVHD. The effect of activated NK cells and $V\alpha24^+V\beta11^+$ NKT cells on these $CD8^+$ T cells remains to be further investigated.

In conclusion, our method for expanding $V\alpha24^+V\beta11^+$ NKT cells derived from CBMNC is easy to perform and may be helpful for future clinical use.

Materials and methods

Human umbilical cord blood

Human umbilical cord blood samples were obtained during normal full-term deliveries after obtaining informed consent. We used samples that were not processed by the Tokyo Cord Blood Bank for therapeutic use because of the small volume (less than 40 mL) or the time elapsed. Cord blood samples were stored at room temperature and processed within 36 h of collection.

αGalCer

αGalCer (KRN7000) was dissolved in DMSO and used at a concentration of 100 ng/mL for cell culture. Control experiments were done with βGalCer, an analogue of αGalCer. αGalCer and βGalCer were kindly provided by Kirin Brewery Co, Ltd. (Gunma, Japan).

Cytokines

Recombinant human IL-15, IL-7 and Flt3-L were purchased from Peprotech (London, UK) and used for cell culture at the indicated concentrations.

Cell culture

CBMNC were isolated by Ficoll-Paque (Sigma, St. Louis, USA) density gradient centrifugation and washed twice with PBS. CBMNC (1×10^6 cells/mL) were suspended in complete RPMI 1640 medium supplemented with 10% heat-inactivated FBS, 0.01 mM nonessential amino acids, 1 mM sodium pyruvate, 100 U/mL penicillin, 100 μg/mL streptomycin and 250 ng/mL amphotericin B, and cultured in 6-well plates (2×10^6 cells/well). IL-15 and/or IL-7 and/or Flt3-L were added at the indicated concentrations, and half of the medium was changed every 4–5 days with or without addition of αGalCer. The number of viable mononuclear cells was counted after Trypan blue staining. The absolute number of cells per well was calculated by multiplying the percentage of each subpopulation of CBMNC, measured by FACS analysis, by the total number of viable mononuclear cells.

Flow cytometric analysis

Cell surface markers were analyzed with a FACS Calibur using Cell Quest software (Becton Dickinson, Mountain View, CA). Fresh or cultured cells were suspended in PBS, incubated with mouse serum to block nonspecific binding, and stained for 20 min on ice with specific FITC-, PE- or allophycocyanin-conjugated mouse monoclonal antibodies (mAb). Anti-CD3, -CD19, -CD1a, -CD4, -CD8α and -TCRαβ mAb were purchased from e-Bioscience (CA, USA). Anti-Vα24 (C15) and anti-Vβ11 (C21) mAb were purchased from Coulter-Immunotech (Marseille, France). Anti-CD56, -CD14, -TCRγδ mAb and isotype controls were purchased from BD Pharmingen (CA, USA). PE- and FITC-conjugated anti-IL-4 and anti-IFN-γ antibodies were also from BD Pharmingen and were used for intracellular staining. Dead cells were stained by propidium iodide and gated out. The CBMNC were gated by forward scatter and side scatter, and then $CD3^+$ cells were analyzed. $CD3^+CD4^+CD8^+$ cells were considered as double-positive cells, but doublet formation had not been formally excluded.

AutoMACS depletion assay

Fresh CBMNC were stained with PE-labeled anti-CD14, anti-CD19, and/or anti-CD1a antibodies and were depleted using anti-PE beads in an AutoMACS magnetic sorting system (Miltenyi Biotec GmbH, Germany). Monocytes, B cells, DC or all of these three antigen-presenting cells were depleted, and the remaining cells were cultured with 50 ng/mL IL-15, 10 ng/mL IL-7, 10 ng/mL Flt3-L and 100 ng/mL αGalCer for 15 days as described above.

Intracellular staining

To detect intracellular expression of IL-4 and IFN-γ, cultured CBMNC were stimulated with 1 ng/mL PMA (Sigma, St. Louis, MO) and 2 μM ionomycin (Sigma) in the presence of 2 μM monensin (Sigma) for 4 h. Cells were then washed twice with PBS containing 0.5% BSA and 0.1% sodium azide (PBS/BSA/Azide) and stained for surface markers using fluorescence-conjugated mAb and ethidium monoazide bromide. Cells were fixed in 4% paraformaldehyde (Wako, Japan) for 20 min at room temperature, washed and permeabilized with PBS/BSA/Azide with 0.5% saponin for 10 min. Cells were then incubated with the anti-IL-4 or IFN-γ mAb for 30 min, washed twice and analyzed in a FACS Calibur.

Cytotoxic assay

Analysis of cytotoxic activity against K562 cells was performed with pre-cultured and post-cultured CBMNC using a non-radioactive cytotoxic assay, CytoTox 96 (LDH release methods; Promega, USA). The effector cells (E) and target cells (T) were mixed to obtain T : E ratios of 1 : 10, 1 : 5 and 1 : 1, and incubated for 4 h in 100 μL phenol red-free RPMI 1640 supplemented with 5% FBS in 96-well plates. Target cells were plated at 2×10^4 cells/well. Analysis and calculation were described elsewhere [27].

Statistics

Results are reported as means ± SD from more than three experiments. Significance levels were determined by analysis of variance (ANOVA) followed by the Dunett post-test for differences in means, using JMP software (SAS Institute Inc.).

Acknowledgements: We thank Dr. N. Watanabe for technical support and Pr. O. Spertini for helpful comments and suggestions on the manuscript. Dr. H. Okada's work in Japan has been supported by CHUGAI Pharma France. This work was supported by a Research Grant on Human Genome, Tissue Engineering (H17-O14) from the Japanese Ministry of Health, Labor and Welfare.

References

1 Godfrey, D. I., Hammond, K. J., Poulton, L. D., Smyth, M. J. and Baxter, A. G., NKT cells: Facts, functions and fallacies. *Immunol. Today* 2000. 21: 573–583.

2 Bendelac, A., Rivera, M. N., Park, S. H. and Roark, J. H., Mouse CD1-specific NK1 T cells: Development, specificity, and function. *Annu. Rev. Immunol.* 1997. 15: 535–562.

3 Kawano, T., Cui, J., Koezuka, Y., Toura, I., Kaneko, Y., Motoki, K., Ueno, H. *et al.*, CD1d-restricted and TCR-mediated activation of Valpha14 NKT cells by glycosylceramides. *Science* 1997. 278: 1626–1629.

4 Cui, J., Shin, T., Kawano, T., Sato, H., Kondo, E., Toura, I., Kaneko, Y. *et al.*, Requirement for Valpha14 NKT cells in IL-12-mediated rejection of tumors. *Science* 1997. 278: 1623–1626.

5 Kawano, T., Nakayama, T., Kamada, N., Kaneko, Y., Harada, M., Ogura, N., Akutsu, Y. *et al.*, Antitumor cytotoxicity mediated by ligand-activated human V alpha24 NKT cells. *Cancer Res.* 1999. 59: 5102–5105.

6 Metelitsa, L. S., Naidenko, O. V., Kant, A., Wu, H. W., Loza, M. J., Perussia, B., Kronenberg, M., Seeger, R. C., Human NKT cells mediate antitumor cytotoxicity directly by recognizing target cell CD1d with bound ligand or indirectly by producing IL-2 to activate NK cells. *J. Immunol.* 2001. 167: 3114–3122.

7 Smyth, M. J., Thia, K. Y., Street, S. E., Cretney, E., Trapani, J. A., Taniguchi, M., Kawano, T. *et al.*, Differential tumor surveillance by natural killer (NK) and NKT cells. *J. Exp. Med.* 2000. 191: 661–668.

8 Baxter, A. G., Kinder, S. J., Hammond, K. J., Scollay, R. and Godfrey, D. I., Association between alphabetaTCR$^+$CD4$^-$CD8$^-$ T-cell deficiency and IDDM in NOD/Lt mice. *Diabetes* 1997. 46: 572–582.

9 Sharif, S., Arreaza, G. A., Zucker, P., Mi, Q. S., Sondhi, J., Naidenko, O. V., Kronenberg, M. *et al.*, Activation of natural killer T cells by alpha-galactosylceramide treatment prevents the onset and recurrence of autoimmune type 1 diabetes. *Nat. Med.* 2001. 7: 1057–1062.

10 Miyamoto, K., Miyake, S. and Yamamura, T., A synthetic glycolipid prevents autoimmune encephalomyelitis by inducing Th2 bias of natural killer T cells. *Nature* 2001. 413: 531–534.

11 Seino, K. I., Fukao, K., Muramoto, K., Yanagisawa, K., Takada, Y., Kakuta, S., Iwakura, Y. *et al.*, Requirement for natural killer T (NKT) cells in the induction of allograft tolerance. *Proc. Natl. Acad. Sci. USA* 2001. 98: 2577–2581.

12 Lee, P. T., Benlagha, K., Teyton, L. and Bendelac, A., Distinct functional lineages of human V(alpha)24 natural killer T cells. *J. Exp. Med.* 2002. 195: 637–641.

13 Exley, M., Garcia, J., Balk, S. P. and Porcelli, S., Requirements for CD1d recognition by human invariant Valpha24$^+$ CD4$^-$CD8$^-$ T cells. *J. Exp. Med.* 1997. 186: 109–120.

14 Nieda, M., Nicol, A., Koezuka, Y., Kikuchi, A., Takahashi, T., Nakamura, H., Furukawa, H. *et al.*, Activation of human Valpha24NKT cells by alpha-glycosylceramide in a CD1d-restricted and Valpha24TCR-mediated manner. *Hum. Immunol.* 1999. 60: 10–19.

15 Takahashi, T., Nieda, M., Koezuka, Y., Nicol, A., Porcelli, S. A., Ishikawa, Y., Tadokoro, K. *et al.*, Analysis of human V alpha 24$^+$ CD4$^+$ NKT cells activated by alpha-glycosylceramide-pulsed monocyte-derived dendritic cells. *J. Immunol.* 2000. 164: 4458–4464.

16 Lin, H., Nieda, M. and Nicol, A. J., Differential proliferative response of NKT cell subpopulations to *in vitro* stimulation in presence of different cytokines. *Eur. J. Immunol.* 2004. 34: 2664–2671.

17 Nishi, N., van der Vliet, H. J., Koezuka, Y., von Blomberg, B. M., Scheper, R. J., Pinedo, H. M. and Giaccone, G., Synergistic effect of KRN7000 with interleukin-15, -7, and -2 on the expansion of human V alpha 24$^+$V beta 11$^+$ T cells *in vitro*. *Hum. Immunol.* 2000. 61: 357–365.

18 van der Vliet, H. J., Nishi, N., Koezuka, Y., von Blomberg, B. M., van den Eertwegh, A. J., Porcelli, S. A., Pinedo, H. M. *et al.*, Potent expansion of human natural killer T cells using alpha-galactosylceramide (KRN7000)-loaded monocyte-derived dendritic cells, cultured in the presence of IL 7 and IL-15. *J. Immunol. Methods* 2001. 247: 61–72.

19 Rogers, P. R., Matsumoto, A., Naidenko, O., Kronenberg, M., Mikayama, T. and Kato, S., Expansion of human Valpha24$^+$ NKT cells by repeated stimulation with KRN7000. *J. Immunol. Methods* 2004. 285: 197–214.

20 Kadowaki, N., Antonenko, S., Ho, S., Rissoan, M. C., Soumelis, V., Porcelli, S. A., Lanier, L. L. and Liu, Y. J., Distinct cytokine profiles of neonatal natural killer T cells after expansion with subsets of dendritic cells. *J. Exp. Med.* 2001. 193: 1221–1226.

21 Woo, S. Y., Jung, Y. J., Ryu, K. H., Park, H. Y., Kie, J. H., Im, S. A., Chung, W. S. *et al.*, *In vitro* differentiation of natural killer T cells from human cord blood CD34$^+$ cells. *Br. J. Haematol.* 2003. 121: 148–156.

22 Ueda, Y., Hagihara, M., Gansuvd, B., Yu, Y., Masui, A., Okamoto, A., Higuchi, A. *et al.*, The effects of alphaGalCer-induced TCRValpha24 Vbeta11(+) natural killer T cells on NK cell cytotoxicity in umbilical cord blood. *Cancer Immunol. Immunother.* 2003. 52: 625–631.

23 Cavazzana-Calvo, M., Hacein-Bey, S., de Saint Basile, G., De Coene, C., Selz, F., Le Deist, F. and Fischer, A., Role of interleukin-2 (IL-2), IL-7, and IL-15 in natural killer cell differentiation from cord blood hematopoietic progenitor cells and from gamma c transduced severe combined immunodeficiency X1 bone marrow cells. *Blood* 1996. 88: 3901–3909.

24 Kennedy, M. K., Glaccum, M., Brown, S. N., Butz, E. A., Viney, J. L., Embers, M., Matsuki, N. *et al.*, Reversible defects in natural killer and memory CD8 T cell lineages in interleukin 15-deficient mice. *J. Exp. Med.* 2000. 191: 771–780.

25 Lodolce, J. P., Burkett, P. R., Boone, D. L., Chien, M. and Ma, A., T cell-independent interleukin 15Ralpha signals are required for bystander proliferation. *J. Exp. Med.* 2001. 194: 1187–1194.

26 Rathmell, J. C., Farkash, E. A., Gao, W. and Thompson, C. B., IL-7 enhances the survival and maintains the size of naive T cells. *J. Immunol.* 2001. 167: 6869–6876.

27 Nagamura-Inoue, T., Mori, Y., Yezhou, Y., Watanabe, N. and Takahashi, T., Differential expansion of umbilical cord blood mononuclear cell derived natural killer cells dependent on the dose of interleukin 15 with Flt3L. *Exp. Haematol.* 2004. 32: 202–209.

28 Rocha, V., Sanz, G. and Gluckman, E., Umbilical cord blood transplantation. *Curr. Opin. Hematol.* 2004. 11: 375–385.

29 Rocha, V., Cornish, J., Sievers, E. L., Filipovich, A., Locatelli, F., Peters, C., Remberger, M. *et al.*, Comparison of outcomes of unrelated bone marrow and umbilical cord blood transplants in children with acute leukemia. *Blood* 2001. 97: 2962–2971.

30 Rocha, V., Labopin, M., Sanz, G., Arcese, W., Schwerdtfeger, R., Bosi, A., Jacobsen, N. *et al.*, Transplants of umbilical-cord blood or bone marrow from unrelated donors in adults with acute leukemia. *N. Engl. J. Med.* 2004. 351: 2276–2285.

31 Takahashi, S., Iseki, T., Ooi, J., Tomonari, A., Takasugi, K., Shimohakamada, Y., Yamada, T. *et al.*, Single-institute comparative analysis of unrelated bone marrow transplantation and cord blood transplantation for adult patients with hematologic malignancies. *Blood* 2004. 104: 3813–3820.

32 Hashimoto, D., Asakura, S., Miyake, S., Yamamura, T., Van Kaer, L., Liu, C., Tanimoto, M. and Teshima, T., Stimulation of host NKT cells by synthetic glycolipid regulates acute graft-*versus*-host disease by inducing Th2 polarization of donor T cells. *J. Immunol.* 2005. 174: 551–556.

33 Fujii, S., Application of natural killer T-cells to posttransplantation immunotherapy. *Int. J. Hematol.* 2005. 81: 1–5.

34 Saikh, K. U., Khan, A. S., Kissner, T. and Ulrich, R. G., IL-15-induced conversion of monocytes to mature dendritic cells. *Clin. Exp. Immunol.* 2001. 126: 447–455.

35 Mohamadzadeh, M., Berard, F., Essert, G., Chalouni, C., Pulendran, B., Davoust, J., Bridges, G. *et al.*, Interleukin 15 skews monocyte differentia-

tion into dendritic cells with features of Langerhans cells. *J. Exp. Med.* 2001. 194: 1013–1020.

36 Hammond, K. J., Pelikan, S. B., Crowe, N. Y., Randle-Barrett, E., Nakayama, T., Taniguchi, M., Smyth, M. J. *et al.*, NKT cells are phenotypically and functionally diverse. *Eur. J. Immunol.* 1999. 29: 3768–3781.

37 Benlagha, K., Weiss, A., Beavis, A., Teyton, L. and Bendelac, A., *In vivo* identification of glycolipid antigen-specific T cells using fluorescent CD1d tetramers. *J. Exp. Med.* 2000. 191: 1895–1903.

38 MacDonald, H. R., Development and selection of NKT cells. *Curr. Opin. Immunol.* 2002. 14: 250–254.

39 Gumperz, J. E., Miyake, S., Yamamura, T. and Brenner, M. B., Functionally distinct subsets of CD1d-restricted natural killer T cells revealed by CD1d tetramer staining. *J. Exp. Med.* 2002. 195: 625–636.

40 Hameg, A., Gouarin, C., Gombert, J. M., Hong, S., Van Kaer, L., Bach, J. F. and Herbelin, A., IL-7 up-regulates IL-4 production by splenic NK1.1$^+$ and NK1.1$^-$ MHC class I-like/CD1-dependent CD4$^+$ T cells. *J. Immunol.* 1999. 162: 7067–7074.

41 Smyth, M. J., Crowe, N. Y., Hayakawa, Y., Takeda, K., Yagita, H. and Godfrey, D. I., NKT cells – conductors of tumor immunity? *Curr. Opin. Immunol.* 2002. 14: 165–171.

42 Ruggeri, L., Capanni, M., Urbani, E., Perruccio, K., Shlomchik, W. D., Tosti, A., Posati, S. *et al.*, Effectiveness of donor natural killer cell alloreactivity in mismatched hematopoietic transplants. *Science* 2002. 295: 2097–2100.

Available online at www.sciencedirect.com
ScienceDirect
Biochemical and Biophysical Research Communications 351 (2006) 853–859
BBRC
www.elsevier.com/locate/ybbrc

Successful immortalization of mesenchymal progenitor cells derived from human placenta and the differentiation abilities of immortalized cells

Xiaohong Zhang [a], Yasushi Soda [b], Kenji Takahashi [a], Yuansong Bai [b], Ayako Mitsuru [a], Koichi Igura [a], Hitoshi Satoh [c], Satoru Yamaguchi [d], Kenzaburo Tani [e], Arinobu Tojo [b], Tsuneo A. Takahashi [a,*]

[a] *Division of Cell Processing, The Institute of Medical Science, The University of Tokyo, 4-6-1 Shirokanedai, Minato-ku, Tokyo 108-8639, Japan*
[b] *Division of Molecular Therapy, Advanced Clinical Research Center, The Institute of Medical Science, The University of Tokyo, Tokyo, Japan*
[c] *Laboratory of Tumor Cell Biology, Department of Medical Genome Sciences, Graduate School of Frontier Sciences, The University of Tokyo, Tokyo, Japan*
[d] *Yamaguchi Hospital, Nishi-Funa, Funabashi, Chiba, Japan*
[e] *Division of Molecular Genetics, Medical Institute of Bioregulation, Kyushu University, Fukuoka, Japan*

Received 3 October 2006
Available online 2 November 2006

Abstract

We reported previously that mesenchymal progenitor cells derived from chorionic villi of the human placenta could differentiate into osteoblasts, adipocytes, and chondrocytes under proper induction conditions and that these cells should be useful for allogeneic regenerative medicine, including cartilage tissue engineering. However, similar to human mesenchymal stem cells (hMSCs), though these placental cells can be isolated easily, they are difficult to study in detail because of their limited life span in vitro. To overcome this problem, we attempted to prolong the life span of human placenta-derived mesenchymal cells (hPDMCs) by modifying hTERT and Bmi-1, and investigated whether these modified hPDMCs retained their differentiation capability and multipotency. Our results indicated that the combination of hTERT and Bmi-1 was highly efficient in prolonging the life span of hPDMCs with differentiation capability to osteogenic, adipogenic, and chondrogenic cells in vitro. Clonal cell lines with directional differentiation ability were established from the immortalized parental hPDMC/hTERT + Bmi-1. Interestingly, hPDMC/Bmi-1 showed extended proliferation after long-term growth arrest and telomerase was activated in the immortal hPDMC/Bmi-1 cells. However, the differentiation potential was lost in these cells. This study reports a method to extend the life span of hPDMCs with hTERT and Bmi-1 that should become a useful tool for the study of mesenchymal stem cells.

Keywords: Placenta; Mesenchymal cells; Immortalization; Differentiation; Telomerase; Bmi-1

Human mesenchymal stem cells (hMSCs) from various sources are able to differentiate into different cell lineages under specific culture conditions [1,2], and have generated a great deal of interest because of their potential use in regenerative medicine. Recently the human placenta, umbilical cord, and amnion have received attention as possible sources of hMSCs because of their easy acquisition with few ethical problems compared to other types of cells [3–6]. Since information necessary for cord blood transplantation (i.e., HLA typing, viral screening, contamination by microorganisms, and examination of diseases in donors and their families) is routinely obtained by cord blood banks, the placenta and cord blood should be two of the safest sources of allogeneic mesenchymal cells for regenerative medicine. In this study, we chose chorionic villi from the fetal part of the human placenta as the mesenchymal cell source.

We have reported that mesenchymal progenitor cells derived from the chorionic villi of the human placenta can differentiate into osteoblasts, adipocytes, chondrocytes,

* Corresponding author. Fax: +81 3 5449 5452.
E-mail address: takahasi@ims.u-tokyo.ac.jp (T.A. Takahashi).

0006-291X/$ - see front matter © 2006 Elsevier Inc. All rights reserved.
doi:10.1016/j.bbrc.2006.10.125

and neural cells under specific induction conditions [6]. These cells can be used for chondrogenic tissue engineering [7], suggesting that hPDMCs could potentially represent a useful cell source for regenerative medicine. However, like hMSCs, hPDMCs proliferate slowly with an average life span of 21 population doublings, which makes the cells difficult to study in detail for possible clinical use. Normal human cells undergo limited cell division in culture and then enter a nondividing state called "senescence" [8]. It is generally accepted that normal human cells senesce because they acquire one or more short dysfunctional telomeres and lack telomerase expression [9]. It has also become clear that other factors such as DNA damage and oxidative stress cause cell growth arrest with a senescent phenotype, independent of telomere length and structure [10]. However, through a process known as ex vivo immortalization, it has become possible to induce primary cells to grow indefinitely in vitro by genetic manipulation [11]. Those processes represent an attractive means of producing large quantities of cells for experimental and therapeutic purposes.

In this study, we investigated life span extension of hPDMCs by lentiviral-mediated hTERT and Bmi-1 transduction. The results indicated that immortalization of hPDMCs required both activation of telomerase and down-regulation of p16 INK4a expression. The hPDMCs with an extended life span could differentiate into osteogenic, adipogenic, and chondrogenic cells in vitro. Eight clonal cell lines were established from immortalized parental hPDMC/hTERT + Bmi-1 and their capabilities for directional differentiation were examined. Interestingly, hPDMC/Bmi-1 showed an extended period of proliferation after long-term growth arrest and telomerase was activated in the immortal hPDMC/Bmi-1 cells; however, the differentiation ability was lost in those cells. Our data suggest that hPDMCs have multipotential differentiation capability and also that transduction with hTERT + Bmi-1 provides a useful method to overcome the short life span of hPDMCs.

Materials and methods

Production of lentiviral vector. To obtain the hTERT-coding lentiviral plasmid pHIV-TERT, a fragment containing hTERT cDNA was excised from PGRN145b (Geron Corp, Menlo Park, CA) with *KpnI* and *SalI*, and subcloned into *NheI* and *XhoI* sites of pCS-CDF-ChG, which coding humanized the R. reniformis GFP (hrGFP) gene. Next, the full-length Bmi-1 cDNA was generated by RT-PCR using primers (forward): 5′-*GCTAGC*AGAAATGCATCGAACAACGAGAATC-3′ (underlined: *NheI* site) and (reverse): 5′-*CTCGAG*TATCAACCAGAAGAAGTTGC TGA-3′ (underlined: *XhoI* site) from total RNA extracted from WI-38 cells. The Bmi-1 PCR product was cloned into pCR4Blunt-TOPO vector using a Zero blunt TOPO PCR cloning kit (Invitrogen, Carlsbad, CA). After confirming the Bmi-1 sequence, the fragment excised with *NheI* and *XhoI* was ligated to pCS-CDF-ChG-PRE digested with *NheI* and *XhoI* (pHIV-Bmi-1). The lentiviral vector stock was produced and the titer was measured as described previously [12].

Isolation, culture, and vector transduction of hPDMCs. The study was approved by the Internal Review Board of our institute. Mesenchymal cells were isolated from chorionic villi by the explant culture method described previously [6]. The migrated cells were regarded as population doubling 0 (PD 0). The hPDMCs were isolated without contamination by maternal cells, which was confirmed by XY chromosome analysis using fluorescence in situ hybridization (FISH) as described previously [6]. hPDMCs at PD 8 were inoculated with the hTERT expression lentiviral vector (hTERT-LV) or Bmi-1 expression lentiviral vector (Bmi-1-LV), or a combination of these two vectors at a multiplicity of infection (MOI) of 2.8 for 3 h to generate hPDMC/hTERT, hPDMC/Bmi-1 or hPDMC/hTERT + Bmi-1 cells.

Telomerase activity and telomere length assay. The telomerase activity was assessed by using a telomere repeat amplification protocol (TRAP) kit (Roche, Mannheim, Germany) according to the manufacturer's instructions. The telomere length was determined by using a Telo TAGGG Telomere Length Assay (Roche) as per the manufacturer's instructions.

Immunohistochemical staining of Bmi-1. The control and transduced cells at PD 10 were fixed with 4% paraformaldehyde and incubated with anti-Bmi-1 monoclonal antibody F6 (Upstate Inc., Lake Placid, NY) (1:200) overnight at 4 °C and Bmi-1 was detected using a diaminobenzidine tetrahydrochloride (DAB) substrate kit (Dako, Kyoto, Japan).

Western blot analysis. Western blotting was performed as described previously [11]. Equal amounts of protein (30 μg) were used for detection. The primary antibodies used were anti-Bmi-1 F6 and anti-β-actin (loading control) (Santa Cruz Biotech, Santa Cruz, CA).

Quantitative PCR. Total RNA was isolated using an RNAeasy mini kit (Qiagen, Tokyo, Japan). Following the manufacturer's protocol, cDNAs were synthesized from 1 μg aliquots of total RNA with Superscript II Reverse Transcriptase (Invitrogen) using the oligo (dT) primer (Invitrogen) in a total volume of 20 μl. Quantitative PCR was done as follows: 95 °C for 10 min, 50 cycles of PCR (95 °C for 15 s and 58 °C for 2 min) using 12.5 μl of 2×TaqMan Master (Roche), each primer at 0.6 μM, a 0.6 μM probe, 1 μl of the RT product, and H_2O to 25 μl. The level of mRNA was normalized by using GAPDH as an internal control. Every reaction was performed in duplicate. The results were analyzed using ABI PRISM 7700 program EDITECTOR 1.6. PCR. Sequences of primers and probes were as follows: hTERT (forward): 5′-ACGGCGACATGGAGA ACAA-3′, (reverse): 5′-CACTGTCTTCCGCAAGTTCAC-3′, probe: CTCCTGCCTTTGGTGGATGATTTCTTGTTG; p16 (forward): 5′-G CCCAACGCACCGAATAGT-3′, (reverse): 5′-CGCTGCCCATCATC ATGC-3′, probe: ACGGTCGGAGGCCGATCCA; p14 (forward): 5′-CC TCGTGCTGATGCTACT-3′, (reverse): 5′-CGCTGCCCATCATCA TGC-3′, probe: TCTAGGGCAGCAGCCGCTTC; GAPDH (forward): 5′-GAAGGTGAAGGTCGGAGTC-3′, (reverse): 5′-GAAGATGGTG ATGGGATTC-3′, probe: GGCTGAGAACGGGAAGCTTG.

Culture of immortalized clonal cells. One hundred hPDMC/hTERT + Bmi-1 cells at PD 20 were plated in a 100-mm diameter dish, and the cultures were maintained in the culture medium until well-defined clones were formed. Then the clones were harvested using sterile cloning rings and replated in a 100-mm diameter dish to form clones again. The clones were harvested and expended for analysis. Eight clonal cell lines were analyzed for osteogenic, chondrogenic, and adipogenic potential.

Osteogenic, chondrogenic, and adipogenic differentiation of hPDMCs. The differentiation potential of prolonged-culture cells was examined using the differentiation-induction protocol and differentiation assay described previously [6].

Results

Characteristics of hPDMCs transfected with hTERT, Bmi-1, or hTERT + Bmi-1

As described previously [6], the hPDMCs had fibroblast-like morphology as shown in Fig. 1Aa. By the FISH assay, 100% XY and 0% XX signals were detected in 500 migrated cells from the placenta of a male baby, indicating that these cells derived from the fetal part of the placenta, i.e., the chorionic villi, without contamination by the maternal part.

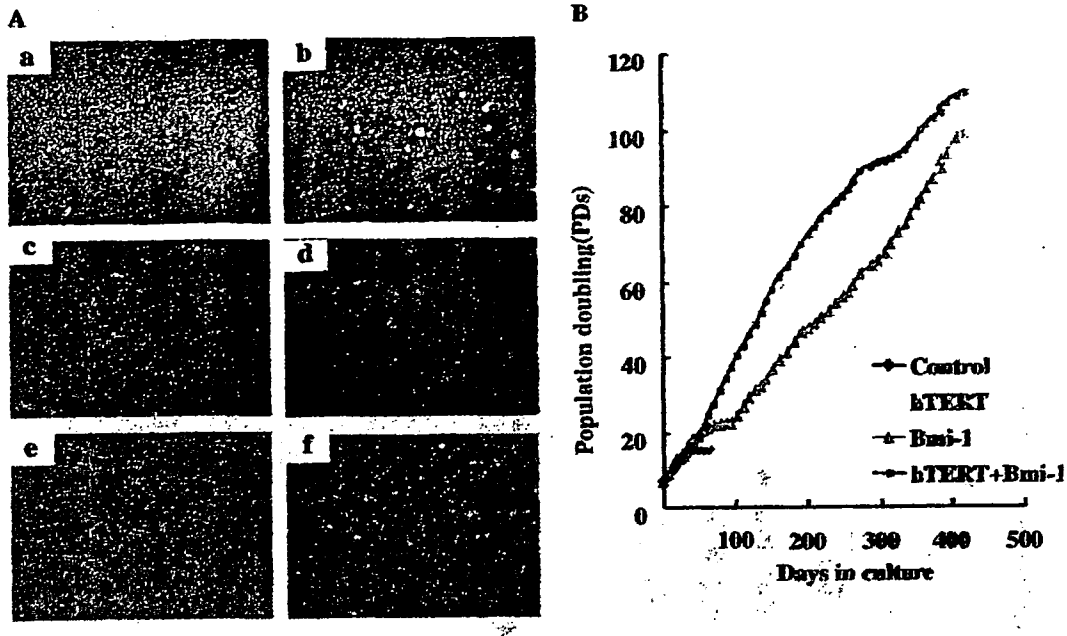

Fig. 1. Morphology and growth change. (A) Morphology of hPDMCs. (a) The control cells at PD 8. (b) The control cells at PD 15. (c) hPDMC/hTERT at PD 15. (d) hPDMC/hTERT+Bmi-1 at PD 20. (e) hPDMC/Bmi-1 at PD 22. Arrowheads indicate smaller, mitotically active cells among large cells. (f) hPDMC/Bmi-1 at PD 40. Magnification 100×. (B) Proliferation curves of control and transduced cells. Control cells (blue), hPDMC/hTERT (yellow), hPDMC/Bmi-1 (green), and hPDMC/hTERT+Bmi-1 (red) are shown. (For interpretation of the references in color in this figure legend, the reader is referred to the web version of this article.)

At PD 8, the hPDMCs were inoculated with hTERT-LV and/or Bmi-1-LV at an MOI of 2.8. The transduction efficiency of hrGFP-LV under the same conditions was shown to be almost 100% by FCM. Until PD 15, the growth rates of these transductants and untransduced hPDMCs were almost the same (Fig. 1B). The control and hPDMC/hTERT cells became broad, flat and stopped replicating (Fig. 1Ab and Ac) indicating that these cells had entered senescence. On the other hand, the cells transduced with hTERT + Bmi-1 and Bmi-1 escaped the replication crisis and proliferated continuously. During the following culture, the proliferation rate of hPDMC/hTERT + Bmi-1 accelerated and the cells became smaller (Fig. 1Ad). The proliferation rate of hPDMC/Bmi-1 became slow at approximately PD 20. However, smaller, mitotically active cells that existed among large cells proliferated when the hPDMCs/Bmi-1 were cultured continuously (Fig. 1Ae). The shape of hPDMC/Bmi-1 became uniform with increasing numbers of passages (Fig. 1Af), indicating that these cells had bypassed the replication crisis. The same results were obtained when the transduced cells at the 1st passage were cultured repeatedly to exclude the possibility that the results were caused by contamination by other types of cells during cell processing. Both hPDMC/hTERT + Bmi-1 and hPDMC/Bmi-1 were maintained in culture for more than 1 yr and continued to proliferate to more than PD 100, suggesting that these cells were immortal (Fig. 1B).

Telomerase activity and telomere length in transduced cells

Telomerase activity was undetectable in control and hPDMC/Bmi-1 cells at PD 15 (Fig. 2A). In contrast, telomerase activity was observed in hPDMC/hTERT at PD 15, and in hPDMC/hTERT + Bmi-1 at PD 15 and 30. Telomerase activity was detected in hPDMC/Bmi-1 at PD 30, indicating that telomerase was induced in hPDMC/Bmi-1 cells after they bypassed growth arrest (Fig. 2B). Telomere length in the control cells decreased with increases of PD, whereas it remained the same in the hPDMC/hTERT, regardless of the increase of PD. Telomeres in hPDMC/Bmi-1 at PD 20 were shorter than in control cells at PD 15, but became longer at PD 30 after bypassing the growth crisis. In hPDMC/hTERT + Bmi-1 telomeres were longer at PD 20 and 30, than at PD 10. Quantitative PCR of telomerase gene expression agreed with the results of the TRAP assay (Fig. 2C). That is, the control cells and hPDMC/Bmi-1 at PD 15 and 20 did not express the hTERT gene, but it was detected in hPDMC/hTERT at PD15 and in hPDMC/hTERT + Bmi-1 at all PDs. In hPDMC/Bmi-1, the hTERT gene was detected at PD 30 and continued to appear at PD 50 (Fig. 2C). These data indicated that activation of telomerase was by activating hTERT transcription in hPDMC/Bmi-1.

Overexpression of Bmi-1 in transduced cells

Overexpression of Bmi-1 was examined by immunohistochemical staining and Western blotting. The nuclei of cells transduced with hTERT + Bmi-1 and Bmi-1 were stained intensely with monoclonal antibody F6 against Bmi-1 (Fig. 3Aa and Ab). Slight nuclear staining in the control cells and hTERT-transduced cells at PD 10 was attributed to endogenous protein (Fig. 3Ac and Ad). The results of Western blotting showed overexpression of

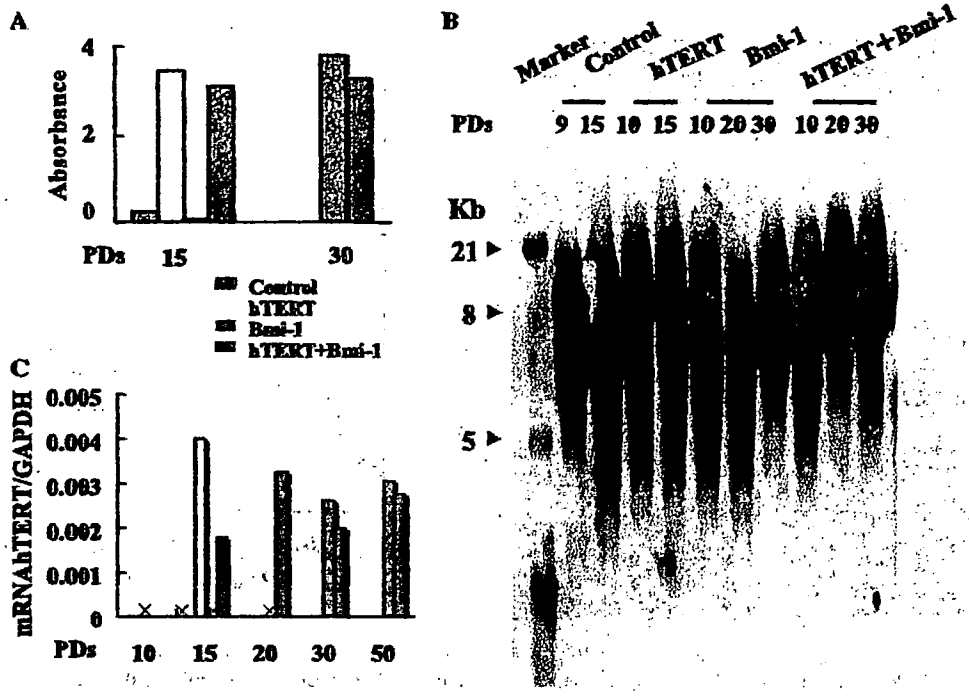

Fig. 2. Detection of telomerase activity. (A) Telomerase activity detected by TRAP assay. No control cells or hPDMC/hTERT cells were harvested at the stage of PD 30. (B) Telomere lengths of control and transduced cells. (C) Quantitative PCR assay shows the expression of hTERT. ×, not detected.

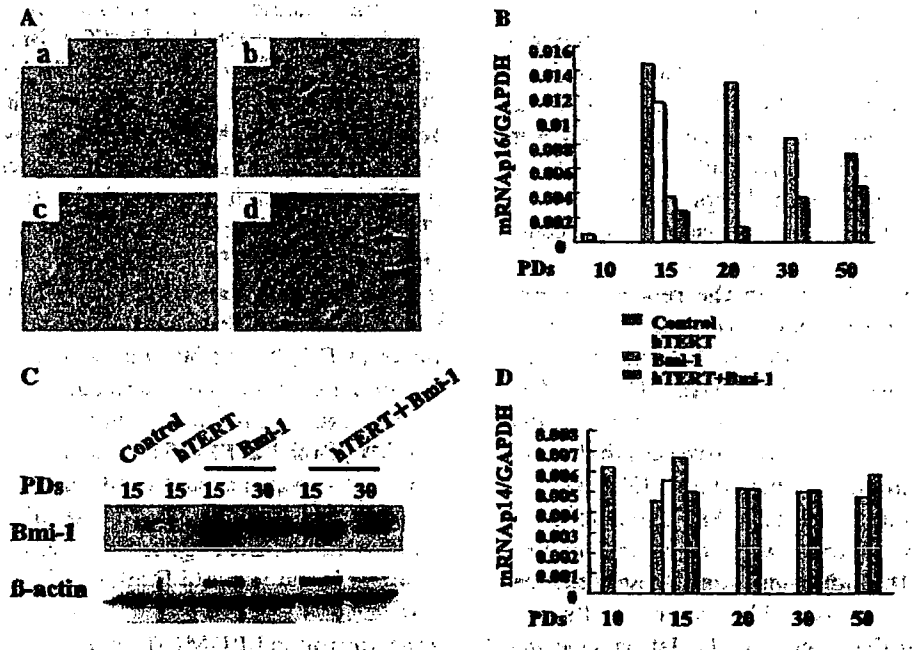

Fig. 3. Detection of overexpressed Bmi-1 and expression of p16 and p14 in hPDMCs. (A) Localization of Bmi-1. Cells at PD 10 were stained with mouse monoclonal antibody. hPDMC/hTERT+Bmi-1 (a) and hPDMC/Bmi-1 (b) were strongly stained in nuclei. Slight nuclear staining in control cells (c) and hPDMC/hTERT (d) was attributable to endogenous protein. Magnification 100×. (B) Western blotting of Bmi-1. No clear band is seen for control cells or hPDMC/hTERT at the senescent stage of PD 15. (C) Expression of p16 detected by quantitative PCR. (D) Expression of p14 detected by quantitative PCR. GAPDH served as an internal control.

Bmi-1 in hPDMC/Bmi-1 and hPDMC/hTERT + Bmi-1 at different PDs. No clear band was observed in the control cells or hPDMC/hTERT at PD 15, which was the senescent stage (Fig. 3B), indicating that expression of Bmi-1 declined in senescent cells. A similar result was shown for WI-38 fibroblasts in a previous report [13].

Down-regulation of p16 extended the life span of hPDMCs, but p14 did not

Bmi-1 is known to down-regulate the expression of two key tumor suppressors, p16 and p14 (p19 in the mouse), which are encoded by a single locus, INK4a [14]. By quan-

titative PCR analysis, we found that p16 expression was up-regulated in the control cells and hPDMC/hTERT at the senescence stage of PD 15 compared to that in the proliferating and young control cells at PD 10. In hPDMC/Bmi-1, the expression of p16 was low at PD 15 but increased at PD 20, then decreased at PD 30 and continued to be down-regulated at PD 50. On the other hand, the expression of p16 was low in hPDMC/hTERT + Bmi-1 at all PDs. However, the level of p16 expression increased as the PD increased (Fig. 3C). The expression level of p14 was the same in the control and transduced cells (Fig. 3D) indicating that extension of the life span of hPDMCs by transduction with Bmi-1 was caused by suppression of the expression of p16, but not p14.

Differentiation potentials of immortalized hPDMCs

Differentiation potentials of hPDMC/hTERT + Bmi-1 and hPDMC/Bmi-1 after prolonged culture were examined. The pellets of hPDMC/hTERT + Bmi-1 cultured for 3 weeks in chondrogenic induction conditions became larger, white, and opaque with glistening and transparency compared to those cultured without induction medium (Fig. 4A, top). The pellets of hPDMCs were positive for toluidine blue and type II collagen (Fig. 4Ba and Bb). Osteogenic differentiation was confirmed by mineralization (Fig. 4Bc) and adipogenic differentiation by lipid vesicles (Fig. 4Bd). However, hPDMC/Bmi-1 showed minimal differentiation potential after bypassing replicative senescence as demonstrated by the pellet size at each PD (Fig. 4A bottom), and no distinct osteogenic or adipogenic differentiation was observed at PD 25 or 30 (data not shown), indicating that the differentiation potential was lost in the cells with extended life spans.

Among eight clonal cell lines, there were four cell lines that showed bi-directional differentiation potential (Fig. 4D), one cell line showed only chondrogenic differentiation, and three cell lines showed no differentiation potential. However, no clonal cell lines differentiated into an adipocyte.

Discussion

In this study, we found that telomerase activity was not sufficient to immortalize hPDMCs. The hPDMCs at PD 15, the senescent stage, showed high expression of p16 compared to younger cells at PD 9. Combination of hTERT and Bmi-1 was shown to be highly effective to extend the life span of hPDMCs (Fig. 1B), indicating that the down-regulation of p16 was the first step necessary for the immortalization of the cells. hPDMC/Bmi-1 went through a long-term growth crisis, after which proliferation started (Fig. 1B). Activation of telomerase was observed in hPDMC/Bmi-1 cells that escaped from the replicative crisis

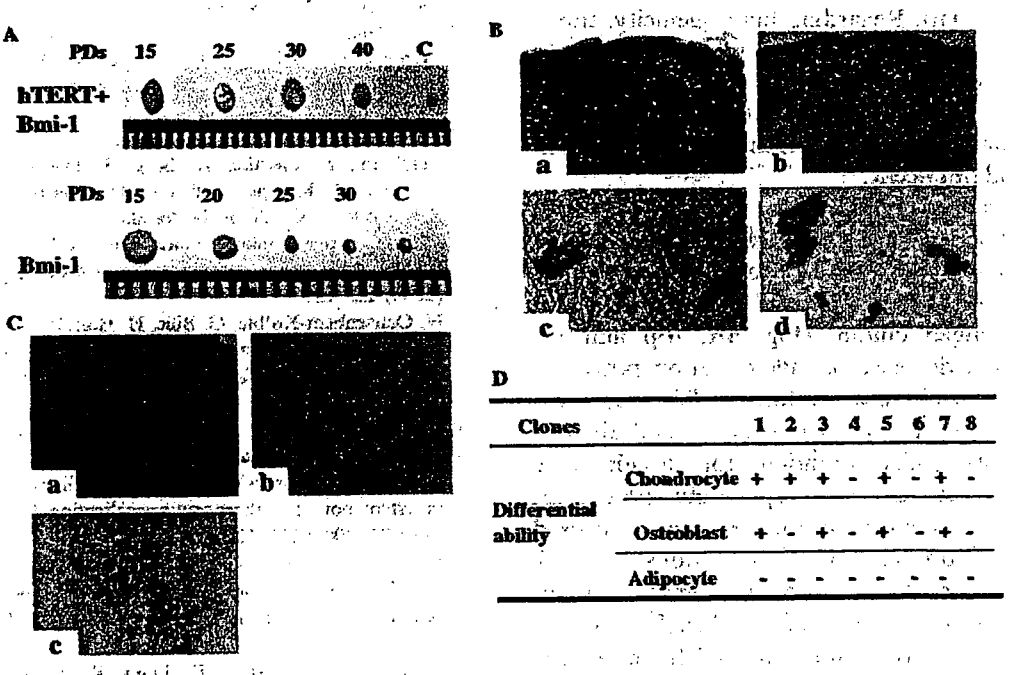

Fig. 4. Pellet culture of immortalized cells at 3 weeks of induction. (A) Top: pellet cultures of hPDMC/hTERT+Bmi-1 at PD 15, 25, 30, and 40, and the induction control (hPDMC/hTERT + Bmi-1 at PD 15). Bottom: pellet cultures of hPDMC/Bmi-1 at PD 15, 20, 25, and 30, and the induction control (hPDMC/Bmi-1 at PD 15). A 1-mm scale ruler is shown. (B) Differentiation potential of hPDMC/hTERT + Bmi-1 at PD 40. Histochemical evidence for chondrogenic ((a) toluidine blue staining, (b) type II collagen immunohistochemical staining), osteogenic ((c) von Kossa staining), and adipogenic ((d) Oil-red-O staining) differentiation. Magnification 100×. (C) Differentiation potential of hPDMC/hTERT + Bmi-1 clone 1. Histochemical evidence for differentiation in two directions, chondrogenic ((a) toluidine blue staining, (b) type II collagen immunohistochemical staining) and osteogenic differentiation ((c) von Kossa staining). Magnification 100×. (D) Differentiation ability of eight clonal cell lines derived from hPDMC/hTERT + Bmi-1 at PD 20.

and were immortalized. Such immortalization may occur in the growth arrest period, probably through the selection of cells that escape from the growth crisis, as reported previously for MRC-5 human lung fibroblasts [15].

We found that hPDMC/hTERT at PD 15 maintained telomere length compared to that in the control cells (PD 10 and 15). It is known that telomerase contributes to the stabilization and/or elongation of telomeres in immortal cells and cancer cells [16]. Telomerase function is regulated by TERT-associated protein and extension cannot be easily achieved if longer telomeres exist in cells [17]. Why telomere length was maintained but not elongated in hPDMC/hTERT at PD 15 may be explained by the long telomere or low function of telomerase in those cells. The expression of p16 was dramatically increased in hPDMC/Bmi-1 at PD 20 and then decreased at PD 30. We assume that many of the cells went into replicative senescence and crisis even though the cells were transfected with Bmi-1; but some infected cells escaped from the crisis, and in these cells the expression of p16 was down-regulated. There are many possible reasons why p16 increased at the crisis stage of hPDMC/Bmi-1, including overexpression of specific genes to induce p16, or no function of Bmi-1 for down-regulation of p16 during the replicative senescence and growth crisis, but we do not have evidence of the cause. A similar phenomenon of p16 down-regulation in immortal hPDMC/Bmi-1 cells was reported for MRC-5 fibroblasts [15]. There was no difference in cell-surface markers of hPDMCs transduced with Bmi-1 and those with a combination of hTERT and Bmi-1 (data not shown). Regarding tumorigenicity, transduced hPDMCs with an extended life span did not form any foci in vitro, and cell division stopped after they reached confluence. They were in the normal cell cycle and had diploid karyotypes (data not shown) indicating that malignant transformation did not occur.

The other purpose of this study was to determine whether cells with a prolonged life span could retain their differentiation potential. Our results showed that the differentiation potential of hPDMC/hTERT + Bmi-1 was maintained after prolonged culture (Fig. 4A, top and B). However, a gradual decrease of differentiation potential, particularly after prolonged culture (>PD 40), was observed in the pellets, i.e., decreases of size and alkaline phosphatase activity under conditions for chondrogenic and osteogenic differentiation, respectively (data not shown). There is a possibility that the decrease was caused by the long-term culture itself reported previously [18,19]. hPDMC/Bmi-1 did not differentiate after bypassing replicative senescence without any change in cell-surface marker of the mesenchymal cells (data not shown). The reason for this limitation is not known, but the possibility that a subtle mutation might have occurred in these cells and inactivated some critical master regulators of differentiation should be considered. Another possibility is that hPDMCs are heterogeneous in their potential for differentiation and only precursor hPDMCs/Bmi-1 cells with low differentiation ability were able to bypass replicative senescence.

Clonal analysis revealed that the differentiation potential was different in the clonal cell lines of hPDMC/hTERT + Bmi-1 (Fig. 4C). The existence of clonal cell lines with directional differentiation proved that the hPDMCs were likely mesenchymal stem cells. However, no cell lines could differentiate into adipocytes, and this was likely caused by long-term culture, similar to extensively cultured bone marrow-derived MSC that lost the ability to differentiate into adipocytes [20].

Our results show that extension of the life span of hPDMCs requires both activation of hTERT and down-regulation of p16. hPDMCs with an extended life span should be useful to study the use of cells for tissue engineering, as well as the mechanism of differentiation.

Acknowledgments

This work was partially supported by a Research Grant on Human Genome, Tissue Engineering (HP-D14, H17-022) from The Japanese Ministry of Health, Labor and Welfare, and Grant-in-Aid from The Japanese Ministry of Education, Culture, Sports, Science and Technology (16390429).

References

[1] M.F. Pittenger, A.M. Mackay, S.C. Beck, R.K. Jaiswal, R. Douglas, J.D. Mosca, M.A. Moorman, D.W. Simonetti, S. Craig, D.R. Marshak, Multilineage potential of adult human mesenchymal stem cells, Science 284 (1999) 143–147.

[2] P.A. Zuk, M. Zhu, P. Ashjian, D.A. De Ugarte, J.I. Huang, H. Mizuno, Z.C. Alfonso, J.K. Fraser, P. Benhaim, M.H. Hedrick, Human adipose tissue is a source of multipotent stem cells, Mol. Biol. Cell. 13 (2002) 4279–4295.

[3] G. Kogler, S. Sensken, J.A. Airey, T. Trapp, M. Muschen, N. Feldhahn, S. Liedtke, R. Sorg, J. Fischer, C. Rosenbaum, S. Greschat, A. Knipper, J. Bender, O. Degistirici, J. Gao, A. Caplan, E.J. Colletti, G. Almeida-Porada, H.W. Muller, E. Zanjani, P. Wernet, A new human somatic stem cell from placental cord blood with intrinsic pluripotent differentiation potential, J. Exp. Med. 200 (2004) 123–135.

[4] N. Ochsenbein-Kolble, G. Bilic, H. Hall, R. Huch, R. Zimmermann, Inducing proliferation of human amnion epithelial and mesenchymal cells for prospective engineering of membrane repair, J. Perinat. Med. 31 (2003) 287–294.

[5] Y.S. Fu, Y.C. Cheng, M.Y. Lin, H. Cheng, P.M. Chu, S.C. Chou, Y.H. Shih, M.H. Ko, M.S. Sung, Conversion of human umbilical mesenchymal stem cells in Wharton's jelly to dopaminergic neurons in vitro: potential therapeutic application for Parkinsonism, Stem Cells 24 (2005) 115–124.

[6] K. Igura, X. Zhang, K. Takahashi, A. Mitsuru, S. Yamaguchi, T.A. Takahashi, Isolation and characterization of mesenchymal progenitor cells from chorionic villi of human placenta, Cytotherapy 6 (2004) 543–553.

[7] X. Zhang, A. Mitsuru, K. Igura, K. Takahashi, S. Ichinose, S. Yamaguchi, T.A. Takahashi, Mesenchymal progenitor cells derived from chorionic villi of human placenta for cartilage tissue engineering, Biochem. Biophys. Res. Commun. 340 (2004) 944–952.

[8] J. Campisi, Replicative senescencese: an old lives' tale? Cell 84 (1996) 497–500.

[9] C.B. Harley, A.B. Futcher, C.W. Greider, Telomeres shorten during ageing of human fibroblasts, Nature 345 (1990) 458–460.

[10] R.D. Ramirez, C.P. Morales, B.S. Herbert, J.M. Rohde, C. Passons, J.W. Shay, W.E. Wright, Putative telomere-independent mechanisms of replicative aging reflect inadequate growth conditions, Genes Dev. 15 (2001) 398–403.
[11] T. Okamoto, T. Aoyama, T. Nakayama, T. Nakamata, T. Hosaka, K. Nishijo, T. Nakamura, T. Kiyono, J. Toguchida, Clonal heterogeneity in differentiation potential of immortalized human mesenchymal stem cells, Biochem. Biophys. Res. Commun. 295 (2002) 354–361.
[12] Y. Bai, Y. Soda, K. Izawa, T. Tanabe, X. Kang, A. Tojo, H. Hoshino, H. Miyoshi, S. Asano, Effective transduction and stable transgene expression in human blood cells by a third-generation lentiviral vector, Gene Ther. 10 (2003) 1446–1457.
[13] K. Itahana, Y. Zou, Y. Itahana, J.L. Martinez, C. Beausejour, J.J. Jacobs, M. van Lohuizen, V. Band, J. Campisi, Control of the replicative life span of human fibroblasts by p16 and the polycomb protein Bmi-1, Mol. Cell Biol. 23 (2003) 389–401.
[14] J.J. Jacobs, K. Kieboom, S. Marino, R.A. DePinho, M. Van Lohuizen, The oncogene and Polycomb-group gene bmi-1 regulates cell proliferation and senescence through the ink4a locus, Nature 397 (1999) 164–168.
[15] L.M. Taylor, A. James, C.E. Schuller, J. Broe, R.B. Lock, Inactivation of p16INK4α, with retention of pRB and p53/21*cip1* function, in human MRC5 fibroblasts that overcome a telomere-independent crisis during immortalization, J. Biol. Chem. 279 (2004) 43634–43645.
[16] N.W. Kim, M.A. Piatyszek, K.R. Prowse, C.B. Harley, M.D. West, P.L.C. Ho, G.M. Coviello, W.E. Wright, S.L. Weinrich, J.W. Shay, Specific association of human telomerase activity with immortal cells and cancer, Science 266 (1994) 2011–2014.
[17] C. Autexier, N.F. Lue, The structure and function of telomerase reverse transcriptase, Annu. Rev. Biochem. 75 (2006) 493–518.
[18] S. Tsutsumi, A. Shimazu, K. Miyazaki, H. Pan, C. Koike, E. Yoshida, K. Takagishi, Y. Kato, Retention of multilineage differentiation potential of mesenchymal cells during proliferation in response to FGF, Biochem. Biophys. Res. Commun. 288 (2001) 413–419.
[19] S. Shi, S. Gronthos, S. Chen, A. Reddi, C.M. Counter, P.G. Robey, C.Y. Wang, Bone formation by human postnatal bone marrow stromal stem cells is enhanced by telomerase expression, Nat. Biotechnol. 20 (2002) 587–591.
[20] P.A. Conget, J.J. Minguell, Phenotypical and functional properties of human bone marrow mesenchymal progenitor cells, J. Cell Physiol. 181 (1999) 67–73.

Available online at www.sciencedirect.com
SCIENCE DIRECT
ELSEVIER
Biochemical and Biophysical Research Communications 340 (2006) 944–952
BBRC
www.elsevier.com/locate/ybbrc

Mesenchymal progenitor cells derived from chorionic villi of +human placenta for cartilage tissue engineering

Xiaohong Zhang [a], Ayako Mitsuru [a], Koichi Igura [a], Kenji Takahashi [a], Shizuko Ichinose [b], Satoru Yamaguchi [c], Tsuneo A. Takahashi [a,*]

[a] *Division of Cell Processing, The Institute of Medical Science, The University of Tokyo (IMSUT), Tokyo, Japan*
[b] *Instrumental Analysis Research Center for Life Science, Tokyo Medical and Dental University, Tokyo, Japan*
[c] *Yamaguchi Hospital, Nishifunabashi, Funabashi, Chiba, Japan*

Received 28 November 2005
Available online 27 December 2005

Abstract

Human mesenchymal stem cells are currently being studied extensively because of their capability for self-renewal and differentiation to various connective tissues, which makes them attractive as cell sources for regenerative medicine. Herein we report the isolation of human placenta-derived mesenchymal cells (hPDMCs) that have the potential to differentiate into various lineages to explore the possibility of using these cells for regeneration of cartilage. We first evaluated the chondrogenesis of hPDMCs in vitro and then embedded the hPDMCs into an atelocollagen gel to make a cartilage-like tissue with chondrogenic induction media. For in vivo assay, preinduced hPDMCs embedded in collagen sponges were subcutaneously implanted into nude mice and also into nude rats with osteochondral defect. The results of these in vivo and in vitro studies suggested that hPDMCs can be one of the possible allogeneic cell sources for tissue engineering of cartilage.

Keywords: Placenta; Mesenchymal cells; Chondrogenesis; Cartilage; Tissue engineering

Mesenchymal stem cells from various sources are capable of differentiating into different cell lineages under proper culture conditions [1–3] and have generated a great deal of interest because of their potential use in regenerative medicine. Recently, the human placenta, umbilical cord, and amnion appeared on the stage in the search for MSCs, because of their easy availability with fewer ethical problems compared to other types of cells [4–6]. Umbilical cord blood contains high numbers of hematopoietic stem/progenitor cells and, like bone marrow, has been used to treat various hematological diseases such as leukemia and aplastic anemia, as well as inherited diseases [7,8]. Cord blood also contains mesenchymal cells and there is a report of the existence of multipotential stem cells (unrestricted somatic stem cells), though the number of MSCs is reported to be much smaller than in bone marrow, and it is also difficult to isolate them consistently [9–11]. The human placenta, umbilical cord, and amnion are discarded after the delivery of infants as medical waste. Since the information necessary for cord blood transplantation, i.e., genetic diseases in donors and their families, viral screening, contamination of microorganisms, etc, needs to be obtained by cord blood banks routinely, cells from the placenta and cord blood should be among the safest of allogeneic cell sources. HLA data such as HLA-A, -B, and -DR of the newborn are also obtained by the banks. Therefore, we chose chorionic villi from the fetal part of the human placenta as a target mesenchymal cell source.

Once cartilage is damaged, little restoration occurs because the tissue has little self-healing capacity. Many attempts have been made to repair defects of cartilage due to trauma, osteochondritis, and other conditions by

* Corresponding author. Fax: +81 3 5449 5452.
E-mail address: takahasi@ims.u-tokyo.ac.jp (T.A. Takahashi).

0006-291X/$ - see front matter © 2005 Elsevier Inc. All rights reserved.
doi:10.1016/j.bbrc.2005.12.091

transplanting chondrocytes or periosteum, and by osteochondral grafts or meniscal allografts [12–15]. However, the results were not satisfactory. The tissue engineering of cartilage has progressed significantly in recent years and bone marrow represents the main source of MSCs for both experimental and clinical studies. However, the use of these cells entails problems such as the necessity of harvesting BM from donors, individual variation [16], limitation to autologous use, and difficulty for hereditary disease patients, all of which underscore the need for alternative sources of autologous and allogeneic MSCs for medical use.

We have reported that mesenchymal progenitor cells from chorionic villi in the human placenta can differentiate into osteoblasts, chondrocytes, adipocytes, and neural cells under different induction conditions in vitro [17], and hPDMCs also have the ability to support the proliferation of hematopoietic stem cells as feeder cells [18]. Therefore, hPDMCs appear to be a possible source of MSCs for use in regenerative medicine. The aim of this study was to analyze the potential for chondrogenic differentiation of hPDMCs and examine whether the hPDMCs could be used as a source of allogeneic mesenchymal cells for tissue engineering of cartilage.

Materials and methods

Isolation and culture of human hPDMCs. This study was approved by the Institutional Review Board of IMSUT. Term placentas were collected after obtaining written informed consent from donors. The processing of the placenta started within 8 h of delivery. To isolate hPDMCs from chorionic villi, the explant culture method was used as described previously [17]. In brief, the amnion and chorionic plate were removed from the placenta, after which the fetal villi were cut into small pieces, washed thoroughly in phosphate-buffered saline (PBS), and then attached to dishes with no coating. Finally, DMEM (low glucose) with 10% FBS and 1% antibiotics/antimycotics was added to the plates. After incubation at 37 °C in a 5% CO_2 atmosphere for 2 or 3 weeks, the cells that migrated were harvested with 0.25% trypsin/1 mM EDTA solution and counted using a hemocytometer. For expansion, the harvested cells were reseeded at a density of 2×10^3 cells/cm^2 in DMEM (low glucose) with 10% FBS and 1% antibiotics/antimycotics, and the culture medium was replaced 2 times every week. The cells used in this study were within 5–15 population doublings (approximately three to six passages).

The human bone marrow-derived mesenchymal cells (hBDMCs) used in this study were purchased from BioWhittaker (Walkersville, MD) and cultured in DMEM (low glucose) with 10% FBS and 1% antibiotic/antimycotics.

Clones of hPDMCs. To analyze the chondrogeneic differentiation of subclones of hPDMCs, the cells were seeded at the density of 1×10^3 cells per 100-mm diameter dish culture in conditioned medium with 10 ng/ml recombinant human basic fibroblast growth factor (bFGF) added as a cloning medium. The culture was maintained in the cloning medium until the formation of well-defined colonies. The subclones were harvested using sterile cloning rings and expanded in the cloning medium.

Flow cytometry. The hPDMCs were harvested using a 1-mM EDTA (pH 7.4) solution. For analysis, cells were stained by combination of antibodies and propidium iodide (PI): FITC-conjugated CD44, CD31, and HLA-class I; PE-conjugated CD73, CD29, CD105, and Tie-2; APC-conjugated CD45, CD34; FITC-mouse IgG1; PE-IgG1, APC-IgG1, and PI. After exposure to labeled antibodies, cells were washed with ice-cold PBS (−) and resuspended in ice-cold PBS (−). The expression of the corresponding cell surface antigen was assayed by FACS Calibur using CELL Quest software (BD). The data were analyzed using FlowJo software (Tree Star, Ashland, OR, USA).

Pellet culture. For chondrocyte differentiation, a pellet culture system was used [19]. Briefly, 2×10^5 cells were placed in a 15-ml polypropylene tube and centrifuged into a pellet. The pellet was cultured at 37 °C with 5% CO_2 in 500 μl of chondrogenic medium containing 10 ng/ml transforming growth factor-β_3 (TGF-β_3) and 500 ng/ml bone morphogenetic protein-2 (BMP-2) in addition to high-glucose DMEM supplemented with 10^{-7} M dexamethasone, 50 μg/ml ascorbate-2-phosphate, 40 μg/ml proline, 100 μg/ml pyruvate, and 50 mg/ml ITS + Premix (6.25 μg/ml insulin, 6.25 μg/ml transferrin, 6.25 ng/ml selenious acid, 1.25 mg/ml BSA, and 5.35 mg/ml linoleic acid). The medium was replaced every 3–4 days for 21 days. The chondrogenic medium without BMP-2 was also employed. In the control, the cells were maintained in the medium without BMP-2, TGF-β_3, and dexamethasone. After 3-week induction, the pellets were embedded in paraffin and cut into 5-μm sections, which were then stained with toluidine blue. For immunohistochemistry, an anti type-II collagen monoclonal antibody was used. The reactivity was detected using a diaminobenzidine tetrahydrochloride (DAB) substrate after incubation with an HRP-linked secondary antibody.

Culture in atelocollagen gel. To examine the chondrogenic differentiation of hPDMCs in a three-dimensional culture system, the cells were cultured in atelocollagen gel (Koken, Tokyo, Japan). The volume ratio of the induction medium to 30% atelocollagen gel was 1:4, and the final cell density was adjusted to 1×10^7/ml. The cell–collagen gel composites were cultured in the chondrogenic media as described above and incubated at 37 °C with 5% CO_2. The culture medium was replaced 2 times every week. After a 3-week culture, the cell–atelocollagen gel composite was embedded in paraffin and cut into 5-μm sections for histological analysis with toluidine blue staining.

RT-PCR. To examine the cartilage-specific gene expression, total RNA was prepared from the pellet and cell–atelocollagen gel composite after induction for 2 weeks. The pellet and cell–atelocollagen gel composite were digested with 3 mg/ml collagenase for 3 and 1 h at 37 °C, respectively. hPDMCs without induction were used as a negative control. Total RNA was extracted by using Trizol-LS following the manufacturer's instructions. RT reaction was performed with a Superscript Kit for 50 min at 42 °C, followed by incubation for 15 min at 72 °C using an oligo-dT primer. For examination of the chondrogenic-related gene expression, PCR amplification was performed by 30 cycles of 94 °C for 30 s, 58 °C for 45 s, and 72 °C for 1 min. PCR products were analyzed by electrophoresis in 2% agarose gel containing ethidium bromide for visualization under UV and photographic recording. PCR primers were made as follows: Sox9 (forward) 5′-GAACGCACATCAAGACGGAG-3′, (reverse) 5′-TCTCGTTGATTTCGCTGCTC-3′ (631 bp product; Z46629); COL2A1 (forward) 5′-TTCAGATATGGAGATGACAATC-3′, (reverse) 5′-AGAGTCCTAGAGTGACTGAG-3′ (472 bp product; L10347); Aggrecan (forward) 5′-AAACCACCTCTGCATTCCAC-3′, (reverse) 5′-CCTCTCTCTCCTTGCAGGTC-3′ (560 bp product; NM013227); COL10A1 (forward) 5′-CACCAGGCATTCCAGGATTCC-3′, (reverse) 5′-AGGTTGTTGGTCTGATAGCTC-3′ (926 bp product; NM009925); BMP-2 (forward) 5′-CAGAGACCC ACCCCCAGCA-3′, (reverse) 5′-CTGTTTGTGTTTGGCTTGAC-3′(688 bp product; NM007553); BMP-6 (forward) 5′-CTCGGGGTTCATAAGGTGAA-3′, (reverse) 5′- ACAGCATAAACATGGGGCTTC-3′ (412 bp product; NM001718); β-actin (forward) 5′-TGACGGGGTCACCCACACTGTGCC-3′, (reverse) 5′-TAGAAGCATTTGCGGTGGACGATG-3′ (660 bp product; NM001101).

Transmission electron microscopic examination. The ultrastructural changes were examined by transmission electron microscopy in the pellets cultured for a week. The cultures were terminated by fixing the pellets with 2.5% glutaraldehyde in 0.1 M PBS for 2 h. The cells were washed overnight at 4 °C in the same buffer and postfixed with 1% OsO_4 buffered with 0.1 M PBS for 2 h. The pellets were dehydrated in a graded series of ethanol and embedded in Epon 812. Ultrathin sections were double-stained with uranyl acetate and lead citrate, and then examined with an H-7100 transmission electron microscope (Hitachi, Hitachinaka, Japan).

Subcutaneous transplantation of hPDMC in collagen sponge into nude mice. Chondrogenesis of hPDMCs in vivo was examined by transplantation of hPDMCs into subcutaneously into nude mice. We chose the collagen sponge (5 mm in diameter by 3 mm in thickness, BD Biosciences 354513) as a scaffold to perform the in vivo experiment because it could be easily inserted did not need to be anchored by covering it with periosteum. One × 10^6 cells in 100 μl medium were seeded into the collagen sponge and the composite was cultured for 2 weeks in chondrogenic medium and then transplanted into subcutaneous pockets of nude mice (5 weeks old). After 3 weeks, the composite was taken out, embedded in paraffin, and cut into 5-μm sections for histological analysis by toluidine blue staining.

Transplantation of hPDMC in collagen sponge into articular osteochondral defect in nude rats. For another experiment, a defect in articular cartilage was created as described previously [20]. Briefly, after nude rats (weight around 300 g) were anesthetized, a 3-cm-long scalp skin cut was made at the midline of the parapaellar skin. The soft tissue was dissected to expose the capsule, the capsule was incised, and the patella was dislocated laterally to expose the patella groove of the femur. A defect, 2 mm in diameter and penetrating the subchondral bone plate, was prepared on the patellar groove of the femur with a microdrill. The lesion was flushed with saline and dried with gauze. The hPDMC-loaded collagen sponge was inserted into the defect. The patella was repositioned, and the medial aspect of the capsule was closed with a nylon suture. The joint was not splinted and the rat was allowed to move freely in a cage. An empty defect served as a control. Six weeks after the surgery, the animals were sacrificed and the femoral condyles were dissected and fixed in 10% neutral-buffered formalin for 24 h. Then 0.5 M EDTA (pH 7.4) was used to decalcify the samples (for ≈7 days). The samples were paraffin-embedded, cut into 5-μm sections, and histology was examined by toluidine blue staining. The presence of human cells in the repaired tissue was confirmed by using an antibody specific for human β-2 microglobulin, a component of the class I antibody complex, as described previously [21]. In brief, the primary antibody of β-2 microglobulin conjugated with FITC was diluted 1:10 and used for staining cells. The reactivity was detected using a new fuchsin substrate system after incubation with an APL-linked anti-FITC secondary antibody.

Reagents. Culture medium and chemicals were purchased from the following companies.

Dulbecco's modified Eagle's medium (DMEM), dexamethasone, ascorbate-phosphate, proline, pyruvate, propidium iodide, and the alkaline phosphatase-conjugated anti-FITC antibody were purchased from Sigma Chemical (St. Louis, MO), fetal bovine serum (FBS) from Moregate BioTech (Bulimba, Australia), antibiotics, antimycotics, and 0.25% trypsin/1 mM EDTA solution from Gibco, Life Technologies (Grand Island, NY), Trizol-LS, oligo-dT primers, and Superscript II from Invitrogen Life Technologies (Carlsbad, CA), recombinant human BMP-2 from Yamanouchi Pharmaceutical (Tokyo, Japan), recombinant human TGF-β_3 from R&D System (Minneapolis, MN), recombinant human basic fibroblast growth factor (bFGF) from PeproTech EC (London, UK), type II collagen antibody from Lab Vision (Fremont, CA), antibodies of CD44, CD73, CD31, HLA-class I, HLA-DR, ITS+ Primix and human β_2-microglobin antibody from BD Biosciences (PharMingen, CA), antibodies of CD29, CD105, and CD34 from Beckman Coulter (Tokyo, Japan), antibody of Tie-2 from Nichirei (Tokyo, Japan), and the horseradish peroxidase (HRP)-linked antibody, new fuchsine substrate system, diaminobenzidine tetrahydrochloride (DAB) substrate, and toluidine blue solution from Dako (Kyoto, Japan).

Results

Isolation, expansion, and characterization of hPDMCs

The average number of hPDMCs that migrated per piece of chorionic villi by the explant culture method was ≈1 × 10^4 cells after 20 days and these cells had fibroblast-like shapes with a heterogeneous cell population (Fig. 1A). The phenotypes of hPDMCs were negative for hematopoietic- and endothelial-related cell antigens, such as CD31, CD34, CD45, CD133, and Tie2. They had high expression of mesenchymal progenitor-cell-related antigens, such as CD29, CD44, CD73, CD105, CD90, and HLA-class I, but not HLA-class DR (Fig. 1B). That hPDMCs were isolated without contamination by maternal cells was confirmed by XY chromosome analysis using FISH as described previously [17]. In subclonal culture, clones were isolated from culture dishes and expanded for the analysis.

Chondrocyte differentiation in pellet culture

When the hPDMCs were pelleted into a micromass and differentiated in serum-free medium in the presence of BMP-2, TGF-β_3, and dexamethasone, condensation of the pellet into a single aggregate was observed on the next day. The condensed pellet grew continuingly during culture for 3 weeks and it became white and opaque, with glistening and transparency (Fig. 2A). The pellet from the culture in the induction medium with TGF-β_3 and dexamethasone was smaller than the pellet from the culture in the medium with BMP-2 (Fig. 2B). Paraffin sections of these pellets showed that cartilage matrix was synthesized. The appearance of metachromatic matrix was demonstrated by toluidine blue staining (Fig. 2C), and type II collagen, the specific protein of chondrocyte, was demonstrated by immunohistochemical staining, indicating the occurrence of chondrogenesis.

RT-PCR was used to examine the expression of genes related to chondrogenic differentiation (Fig. 3A), such as Sox9, a major regulator of cartilage-specific genes. Expression of COL2A1, aggrecan, COL10A1, BMP-2, and BMP-6 was detected in the pellets cultured for 2 weeks. TEM examination showed that the cells in the 1-week cultured pellet were oblong with large, euchromatic, ovoid nuclei, and filled with endoplasmic reticula. These cells produced large quantities of extracellular fibers (Fig. 3B).

The pellets of cultured hBDMCs and hPDMCs were similar in size and weight after 3 weeks of induction (Figs. 4A and B). Moreover, chondrogenic differentiation analysis of subclones showed that they grew glistening and transparent (Fig. 4C), indicating that they had potential for chondrogenic differentiation.

Chondrogenic differentiation of hPDMCs in atelocollagen gel

The cell–atelocollagen gel became white, glistening, and harder than the original gel after 3 weeks of culture (Fig. 5A). In histological examination, metachromatic territorial matrixes were observed in atelocollagen gel stained by toluidine blue (Fig. 5B, top). Cells with lacuna formation were examined in the newly formed matrix (Fig. 5B, bottom). RT-PCR confirmed the expression of genes related to the chondrogenic differentiation of hPDMCs in atelocollagen gel after 2 weeks of culture (Fig. 5C).